High-Resolution Solid-State NMR of Quadrupolar Nuclei

Philip J. Grandinetti

Ohio State University

Columbus, OH, USA

http://www.grandinetti.org

Tutorial Lecture presented at the

Bruker User's Meeting

Breckenridge, Colorado

July 2007

The Big Picture

Allowed Nuclear Multipole Moments as a function of Spin I

	$l=0$	$l=1$	$l=2$	$l=3$	$l=4$
Spin	monopole	dipole	quadrupole	octapole	hexadecapole
$I=0$	electric	0	0	0	0
$I=\frac{1}{2}$	electric	magnetic	0	0	0
$I=1$	electric	magnetic	electric	0	0
$I=\frac{3}{2}$	electric	magnetic	electric	magnetic	0
$I=2$	electric	magnetic	electric	magnetic	electric

Nuclear Magnetic Dipole Moment couples to magnetic field

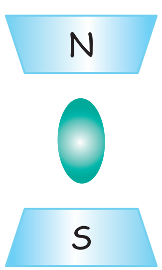

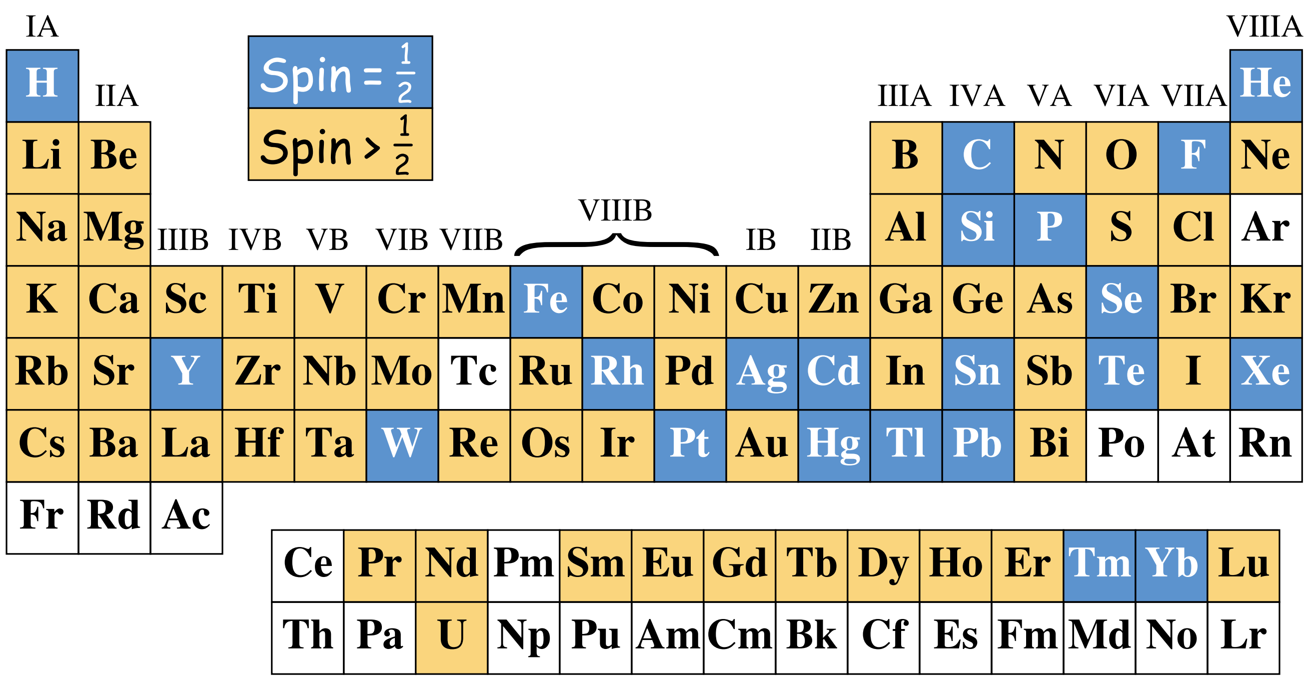

Nuclear Electric Quadrupole Moment couples to electric field gradient

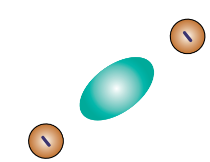

NMR of Quadrupolar Nuclei
Is there a Problem?

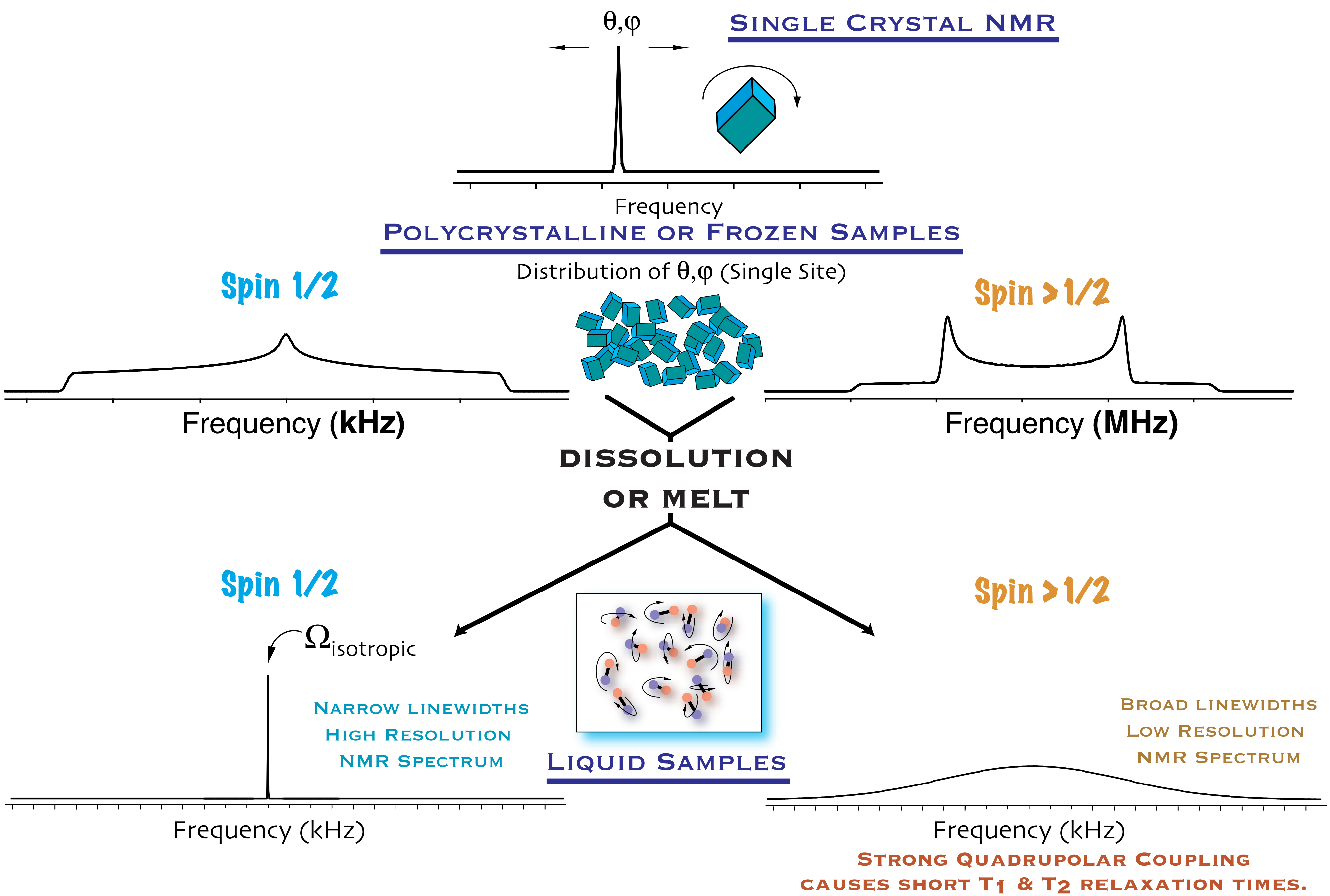

Perturbation expansion of NMR transition frequency

$$\Omega(\theta,\phi) = \Omega^{(0)} + \Omega^{(1)}(\theta,\phi) + \underbrace{\Omega^{(2)}(\theta,\phi) + \Omega^{(3)}(\theta,\phi) + \cdots}_{\text{Quadrupolar Coupling}}$$

$\Omega^{(0)}$: Zeeman Coupling

$\Omega^{(1)}(\theta,\phi)$: Chemical Shift, J-Coupling, Dipolar Coupling, Quadrupolar Coupling

$\Omega^{(2)}(\theta,\phi) + \Omega^{(3)}(\theta,\phi) + \cdots$: Quadrupolar Coupling

Zeroth-Order

$$\Omega^{(0)} = \omega_0 = -\gamma B_0$$

(0 to hundreds of MHz)

First-Order Correction

$$\Omega^{(1)}(\theta,\phi) = \Omega^{(1)}_{iso}(I,m_i,m_f) + \sum_{k=-2}^{2} c^{(1)}_{2,k}(I,m_i,m_f)\ Y_{2,k}(\theta,\phi)$$

ω_q (0 to Tens of MHz)

$$\omega_q = \frac{6\pi C_q}{2I(2I-1)}$$

Second-Order Correction

$$\Omega^{(2)}(\theta,\phi) = \Omega^{(2)}_{iso}(I,m_i,m_f) + \sum_{k=-2}^{2} c^{(2)}_{2,k}(I,m_i,m_f)\ Y_{2,k}(\theta,\phi) + \sum_{k=-4}^{4} c^{(2)}_{4,k}(I,m_i,m_f)\ Y_{4,k}(\theta,\phi)$$

ω_q^2/ω_0 (0 to hundreds of kHz)

Third-Order Correction

$$\Omega^{(3)}(\theta,\phi) = \Omega^{(3)}_{iso}(I,m_i,m_f) + \sum_{k=-2}^{2} c^{(3)}_{2,k}(I,m_i,m_f)\ Y_{2,k}(\theta,\phi) + \sum_{k=-4}^{4} c^{(3)}_{4,k}(I,m_i,m_f)\ Y_{4,k}(\theta,\phi) + \sum_{k=-6}^{6} c^{(3)}_{6,k}(I,m_i,m_f)\ Y_{6,k}(\theta,\phi)$$

ω_q^3/ω_0^2 (0 to hundreds of Hz)

Higher Order Effects of Quadrupolar Nuclei on NMR

Nuclear Magnetic Dipole Moment couples to magnetic field

Nuclear Electric Quadrupole Moment couples to electric field gradient

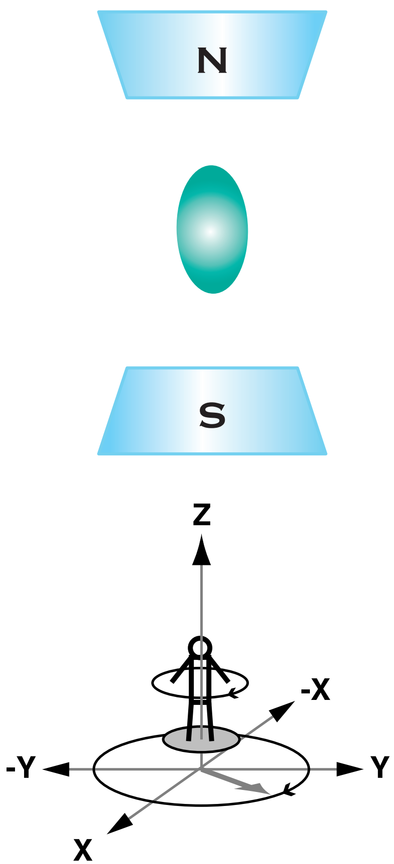

+

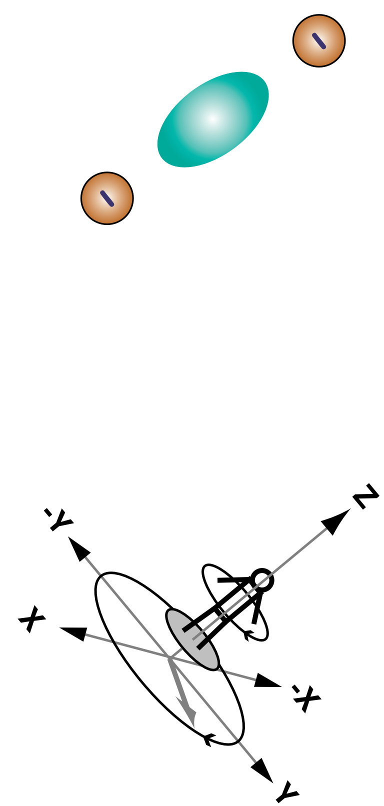

=

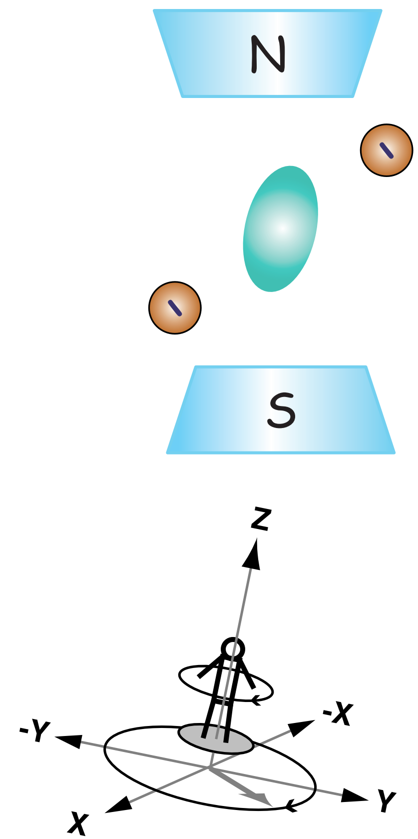

M ⟶ -M TRANSITIONS ARE UNAFFECTED BY FIRST-ORDER QUADRUPOLAR SPLITTING

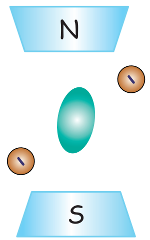

ZEEMAN

QUADRUPOLAR INTERACTION

	0TH	1ST	2ND	3RD

SINGLE QUANTUM TRANSITIONS

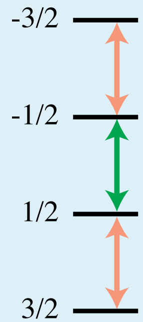

$$\Omega_{ST_-}(\theta,\phi) = \Omega^{(0)} + \Omega^{(1)}_{ST_-}(\theta,\phi) + \Omega^{(2)}_{ST}(\theta,\phi) + \Omega^{(3)}_{ST_-}(\theta,\phi) + \cdots$$

$$\Omega_{CT}(\theta,\phi) = \Omega^{(0)} + 0 + \Omega^{(2)}_{CT}(\theta,\phi) + 0 + \cdots$$

$$\Omega_{ST_+}(\theta,\phi) = \Omega^{(0)} + \Omega^{(1)}_{ST_+}(\theta,\phi) + \Omega^{(2)}_{ST}(\theta,\phi) + \Omega^{(3)}_{ST_+}(\theta,\phi) + \cdots$$

DOUBLE QUANTUM TRANSITIONS

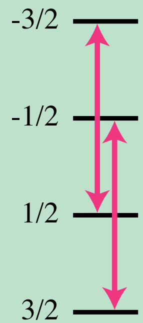

$$\Omega_{2Q_-}(\theta,\phi) = 2\Omega^{(0)} + \Omega^{(1)}_{2Q_-}(\theta,\phi) + \Omega^{(2)}_{2Q_-}(\theta,\phi) + \Omega^{(3)}_{2Q_-}(\theta,\phi) + \cdots$$

$$\Omega_{2Q_+}(\theta,\phi) = 2\Omega^{(0)} + \Omega^{(1)}_{2Q_+}(\theta,\phi) + \Omega^{(2)}_{2Q_+}(\theta,\phi) + \Omega^{(3)}_{2Q_+}(\theta,\phi) + \cdots$$

TRIPLE QUANTUM TRANSITIONS

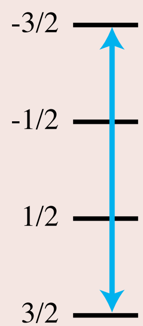

$$\Omega_{3Q}(\theta,\phi) = 3\Omega^{(0)} + 0 + \Omega^{(2)}_{3Q}(\theta,\phi) + 0 + \cdots$$

Single Crystal (and Goniometer Probe) Available?

Vosegaard, Skibsted, Bildsøe, and Jakobsen, *J. Magn. Reson. A*, **122**, 111-119(1996)

Single Crystal ^{87}Rb NMR of $RbClO_4$

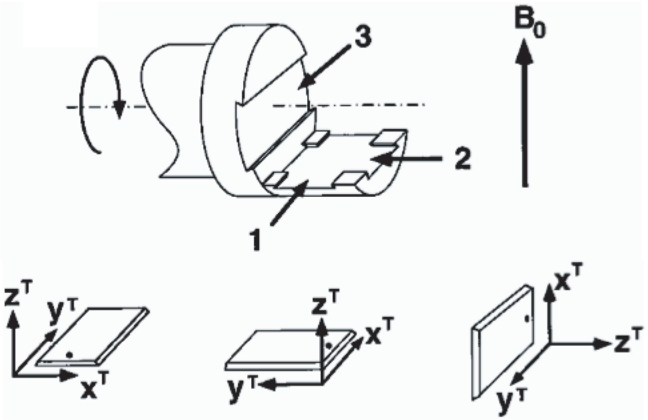

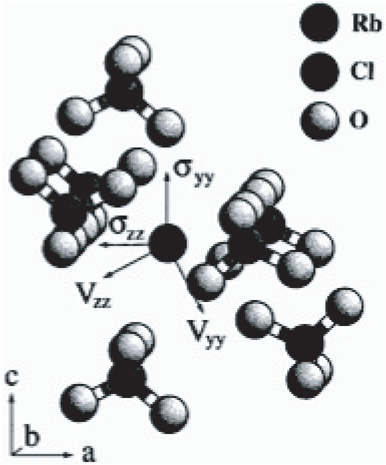

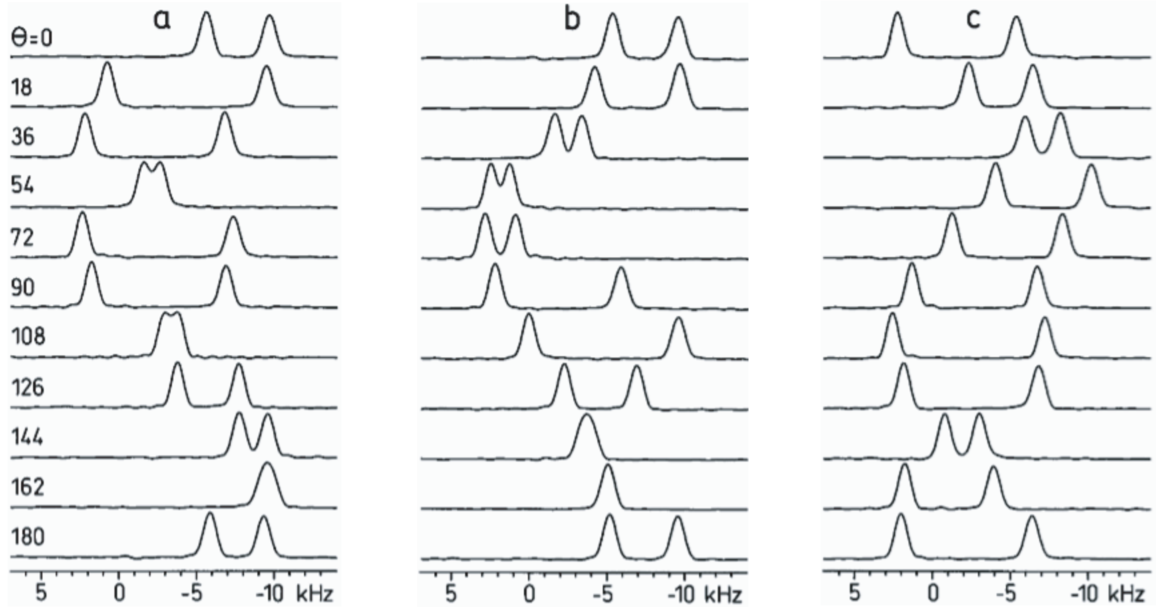

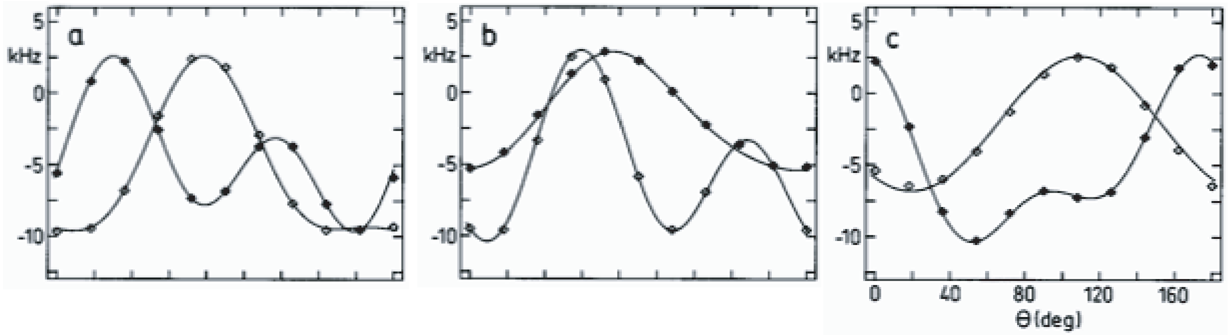

Crystal	Site	Method	C_Q (MHz)	η_Q	δ_σ (ppm)	η_σ	δ_{iso} (ppm)[a]	ψ (degree)	χ (degree)	ξ (degree)	Reference
$RbClO_4$	—	Single-crystal	3.30 ± 0.04	0.21 ± 0.03	13.8 ± 1.5[b]	0.61 ± 0.24[b]	−13.7 ± 0.6[b]	94 ± 14	28 ± 4	87 ± 5	This work
		MAS	3.29 ± 0.05	0.20 ± 0.03	13.5 ± 1.0	0.32 ± 0.20	−13.1 ± 0.3	98 ± 15	34 ± 5	69 ± 20	(7)
		Static	3.24 ± 0.06	0.19 ± 0.06	14 ± 2	0.5 ± 0.3	−14.3 ± 1.8	112 ± 6[c]	28.8 ± 1.5[c]	16 ± 4[c]	(3)

POLYCRYSTALLINE SAMPLES

INTEGER SPINS ^{2}D(I=1), ^{14}N(I=1), ^{10}B(I=3), ^{6}Li(I=1)

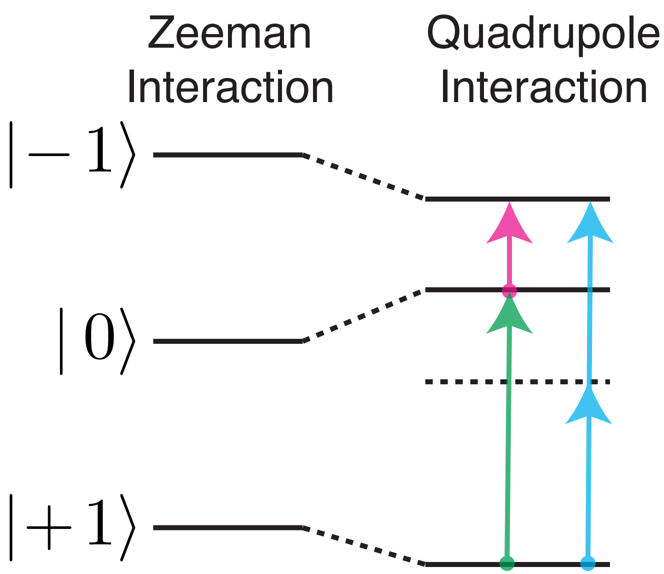

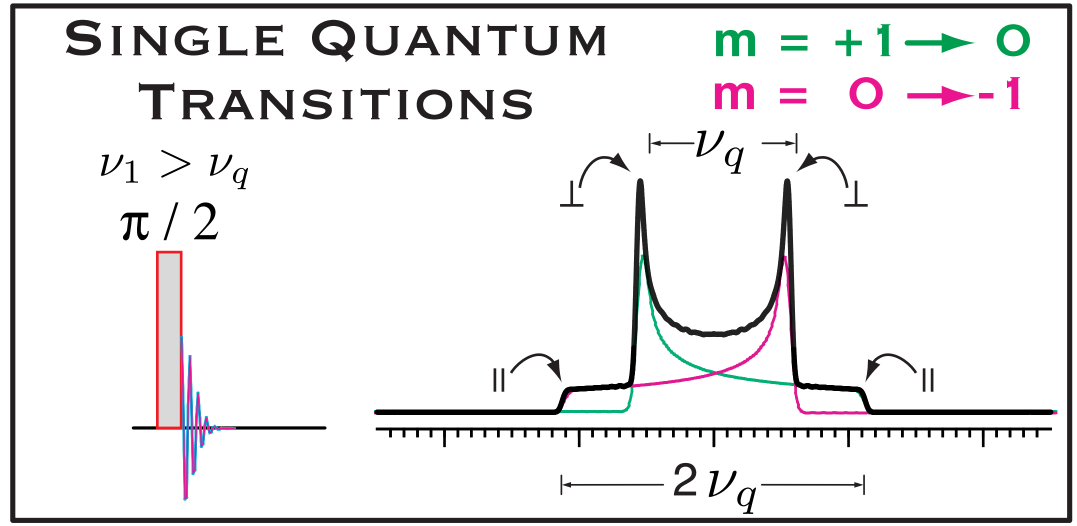

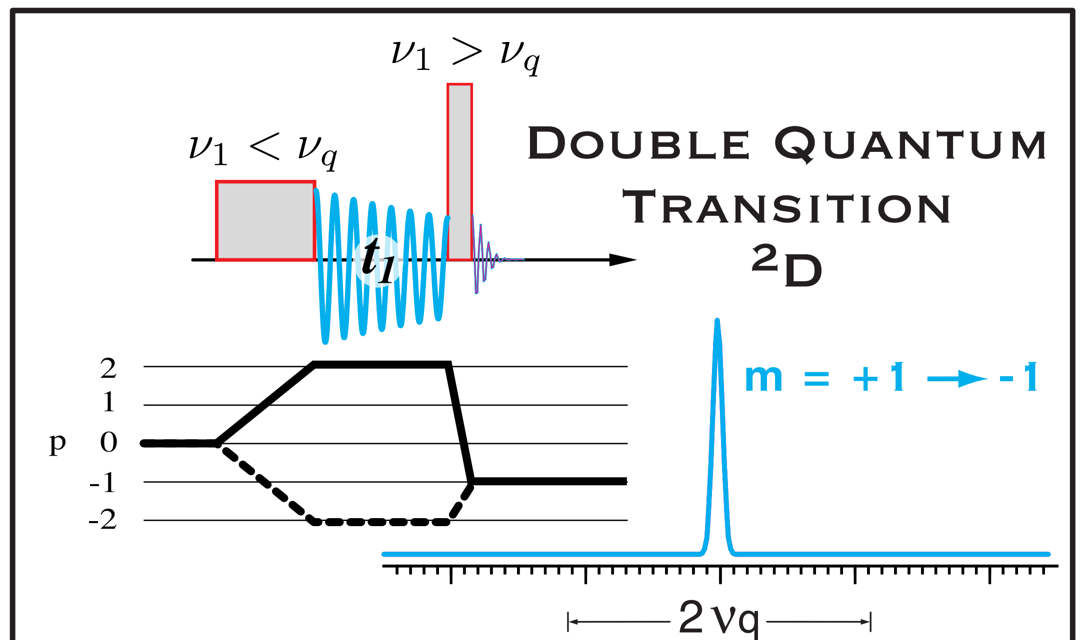

VEGA, SHATTUCK, AND PINES,
Phys. Rev. Lett., **37**, 43-46 (1976)

Half-Integer Spins: Narrow Central Transition, But MAS is Inadequate

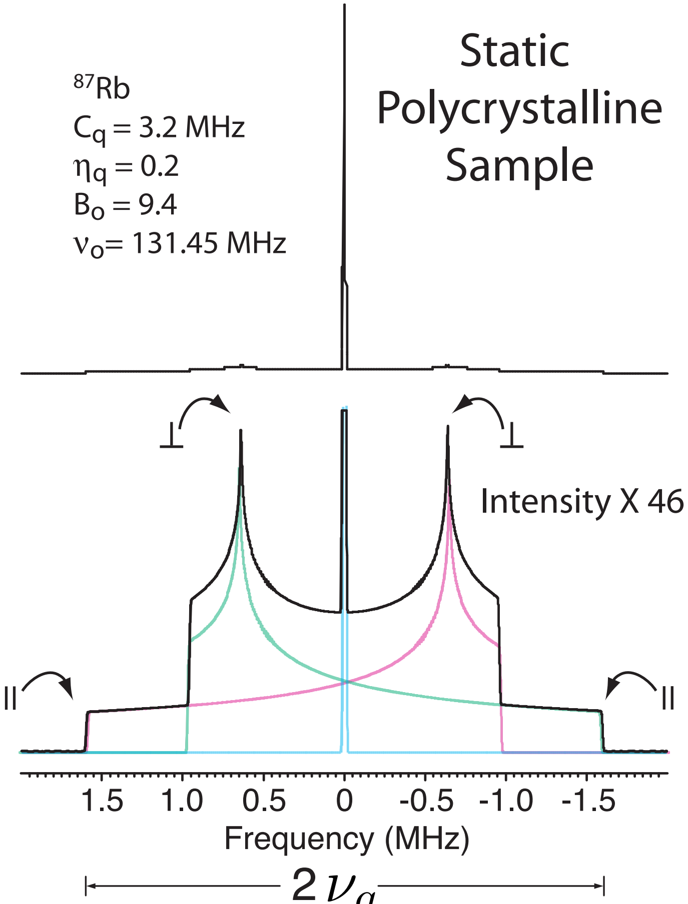

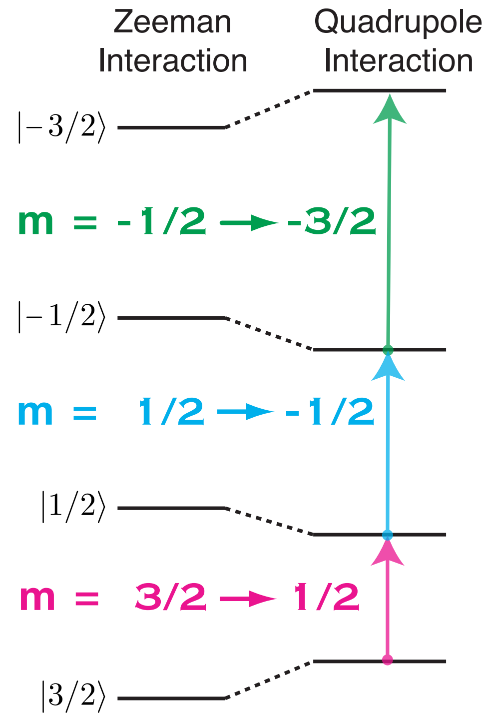

$$\nu_q = \frac{3Cq}{2I(2I-1)}$$

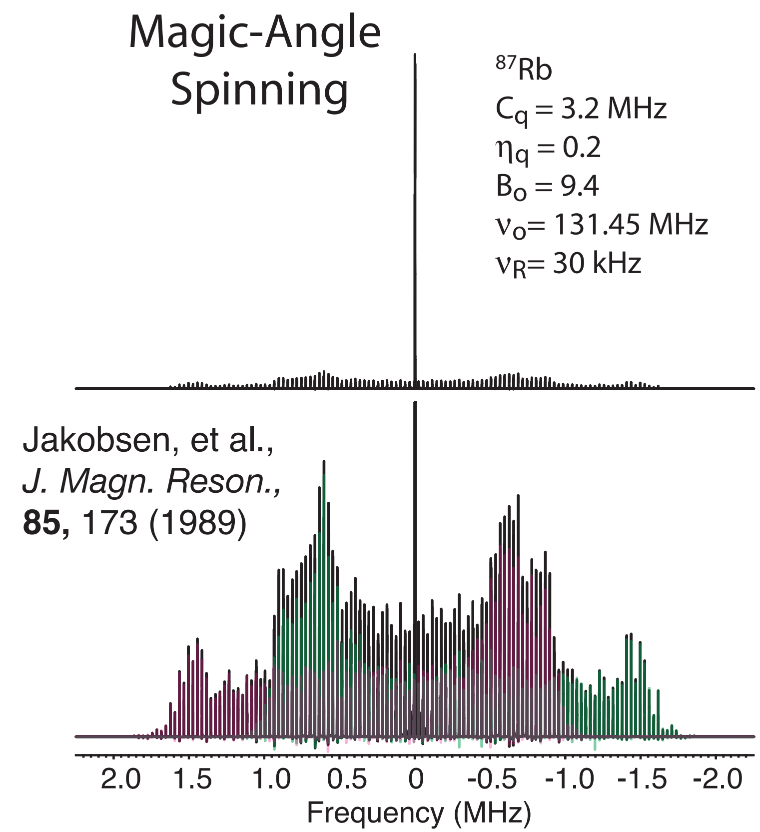

Central Transition

Unaffected by First Order Quadrupolar splitting

m = 1/2 → -1/2

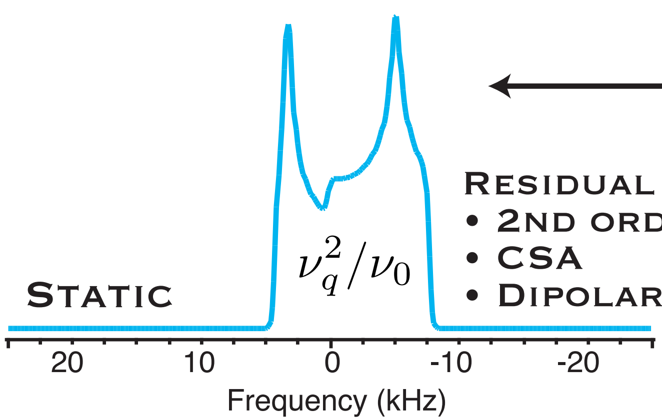

Residual Linewidth
- 2nd order Quad.
- CSA
- Dipolar Couplings

Residual Linewidth
- 2nd order Quad.

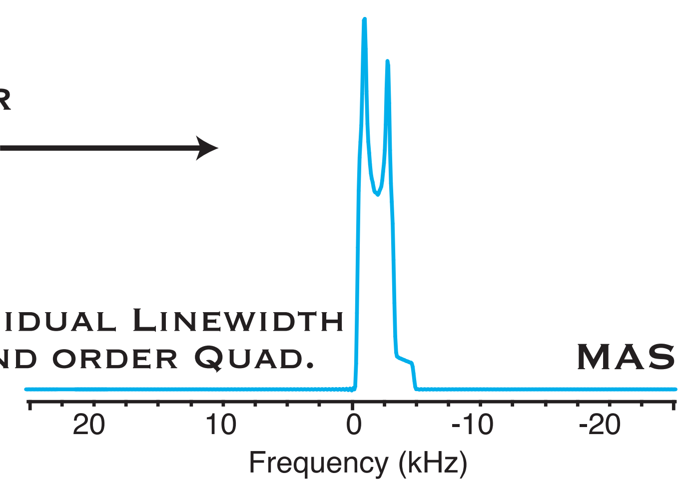

Central Transition Nutation Frequency

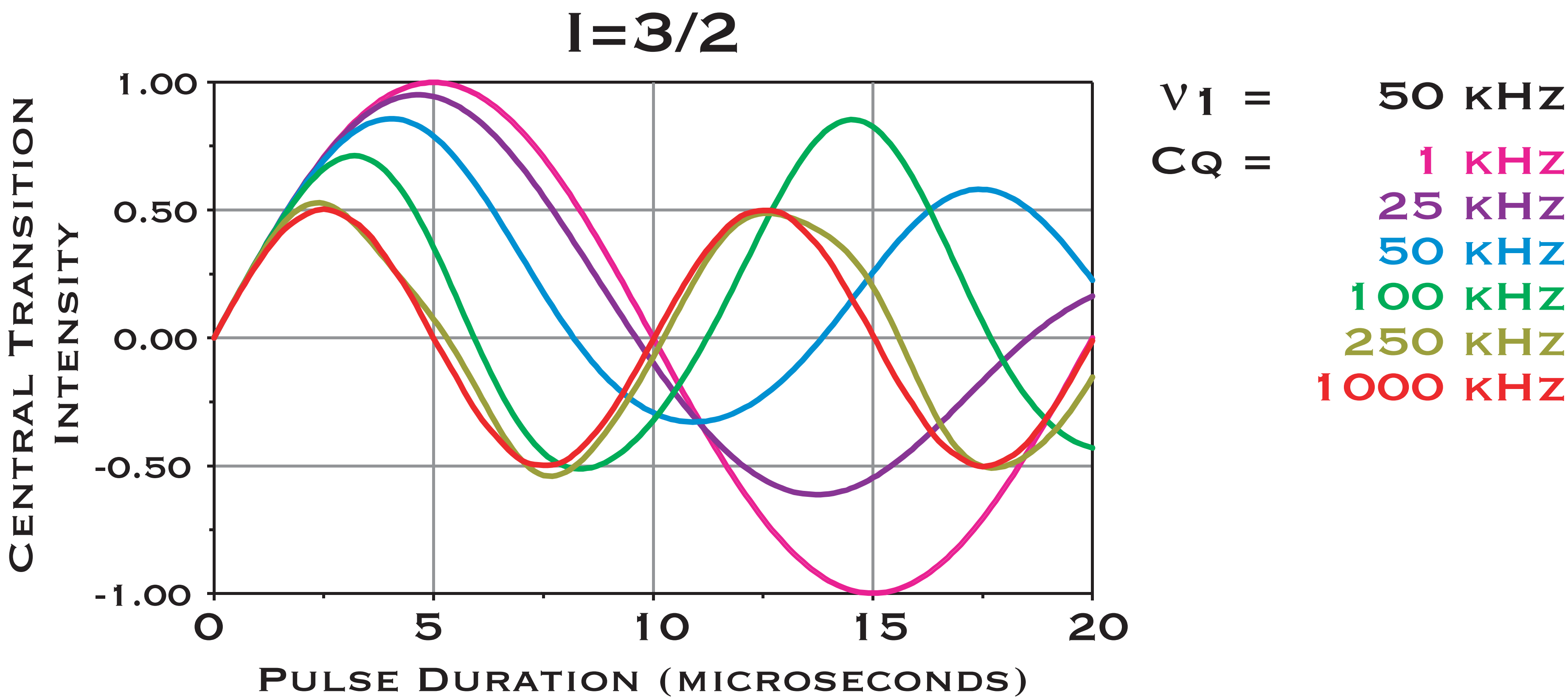

In the limit that $\omega_1 \ll \omega_q$ the effective central transition nutation frequency becomes ...

$$(I + 1/2)\ \omega_1$$

Magic-Angle Spinning:

Great for spin 1/2, but for spin >1/2?

Spin 1/2

^{13}C NMR Spectrum of p-anisic acid

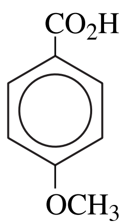

Static

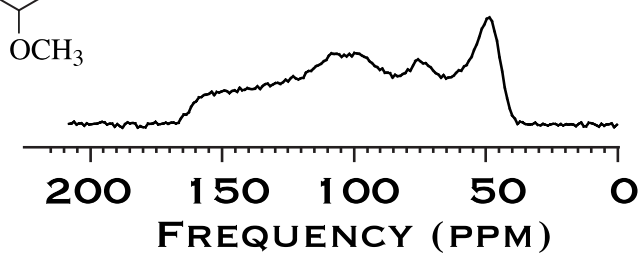

MAS

Narrow linewidths

High Resolution

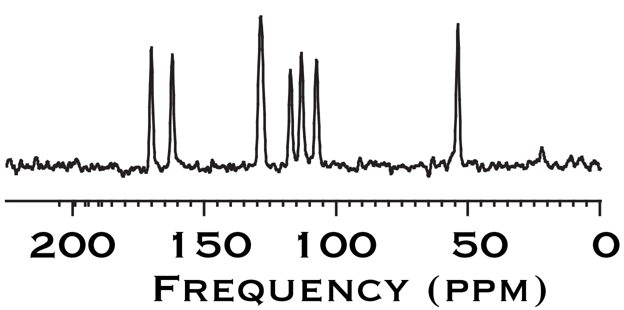

Spin 3/2

^{87}Rb NMR Central Transition Spectrum of $RbNO_3$

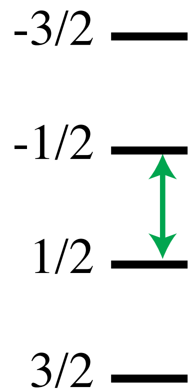

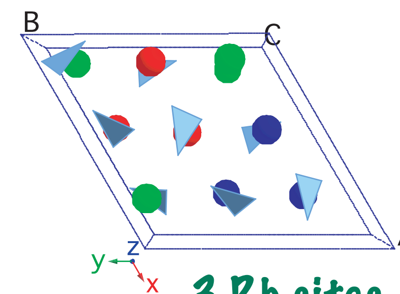

3 Rb sites

Static

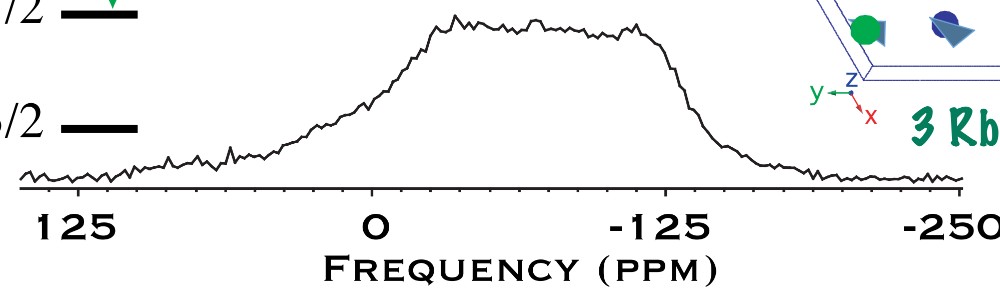

MAS

Broad linewidths

Low Resolution from residual anisotropy, not short relaxation times!

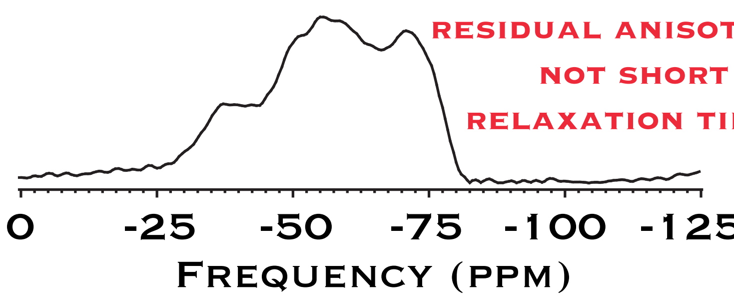

Variable Angle Spinning: Spin 1/2 Nuclei

Variable-Angle Spinning Spectra as a Function of Angle

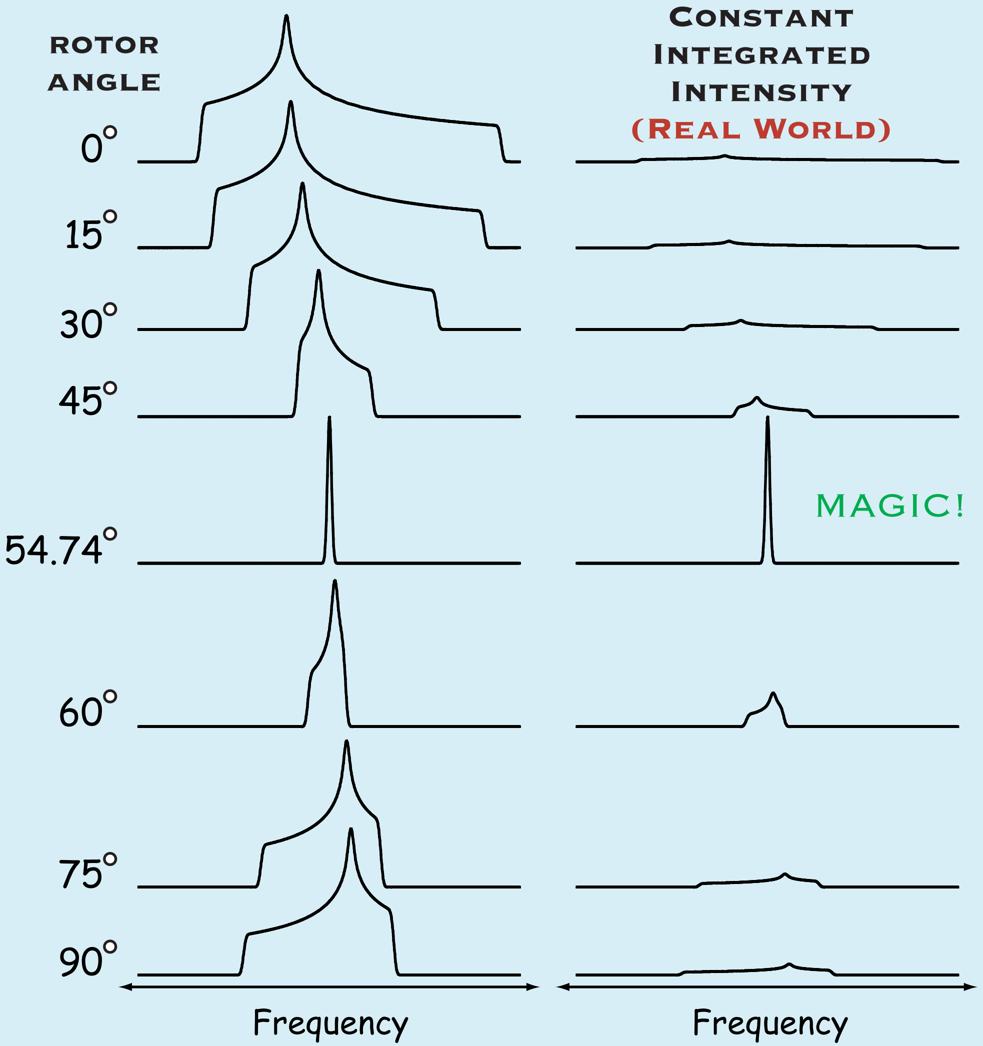

Magic-Angle Spinning Spectra as a Function of Spinning Speed

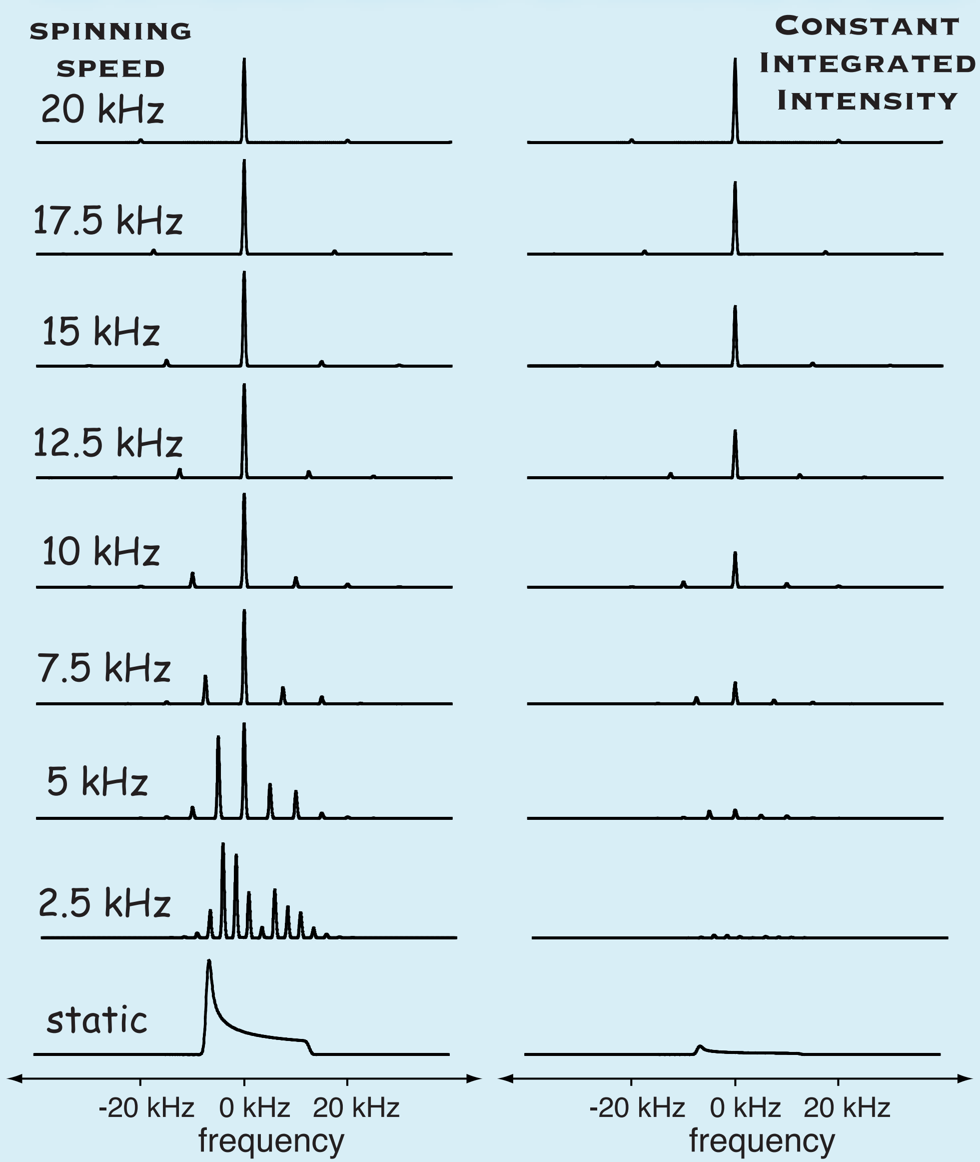

Variable Angle Spinning: Spin > 1/2 (Quadrupolar) Nuclei

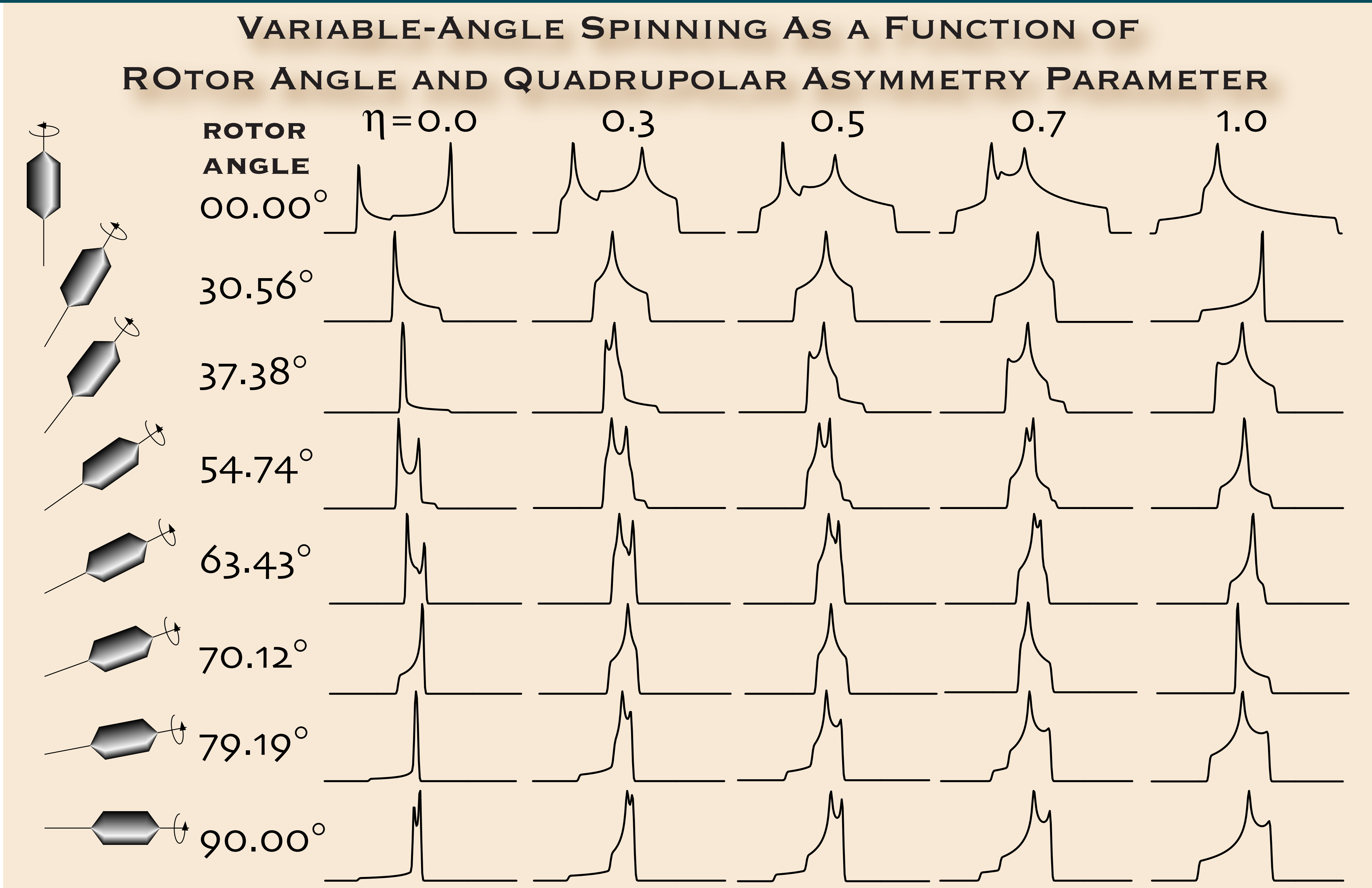

Ganapathy, Schramm, and Oldfield, *J. Chem. Phys.*,*1982*, *77*, *4360*

One Solution: Really High magnetic fields

2nd-order broadenings are inversely proportional to magnetic field strength

^{27}Al MAS spectra of aluminoborate $9Al_2O_3 + 2B_2O_3$ (A_9B_2) compound from 14 to 40 T.

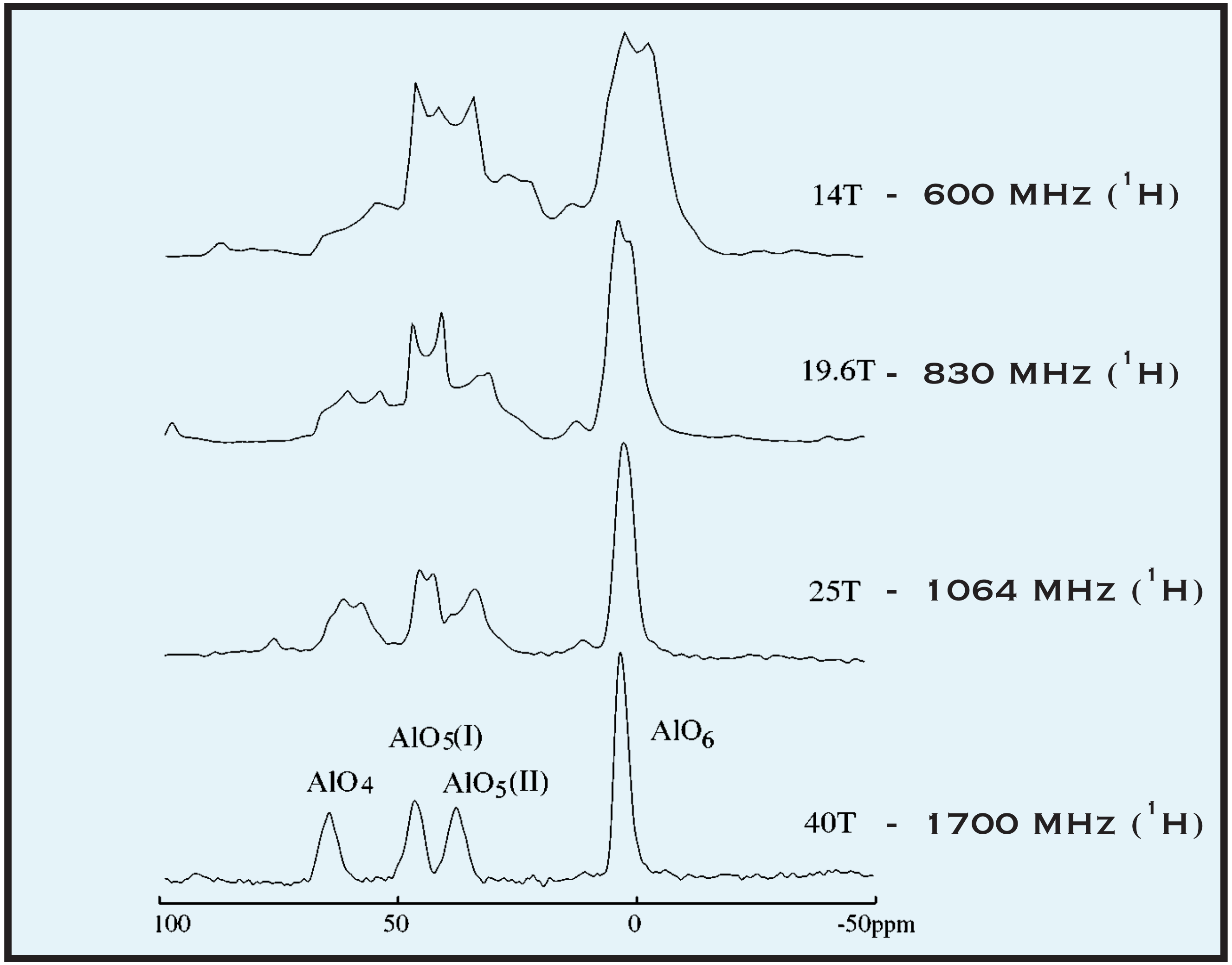

Gan,* Gor'kov, Cross, Samoson, and Massiot **J. AM. CHEM. SOC. 2002**, *124*, 5634- 5635

Another Solution: Be Clever
Averaging Anisotropy of Rank ℓ

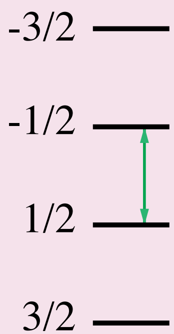

Central Transition

	0th	1st	2nd	3rd	
$\Omega_{CT}(\theta,\phi) =$	$\Omega^{(0)} +$	0	$+\,\Omega^{(2)}_{CT}(\theta,\phi)\ +$	0	$+\cdots$

$$\Omega^{(2)}(\theta,\phi) = \Omega^{(2)}_{iso}(I,m_i,m_f) + \sum_{k=-2}^{2} c^{(2)}_{2,k}(I,m_i,m_f)\ Y_{2,k}(\theta,\phi) + \sum_{k=-4}^{4} c^{(2)}_{4,k}(I,m_i,m_f)\ Y_{4,k}(\theta,\phi)$$

<u>Symmetry</u>

$\boxed{\ell}$ $\langle A_{\ell,m}\rangle = 0$

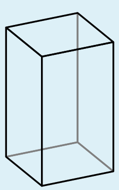

Tetragonal (D4)

$\ell =$	0	1	2	3	4	5	6	7	8	9	10

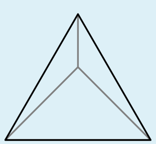

Tetrahedral (T)

$\ell =$	0	1	2	3	4	5	6	7	8	9	10

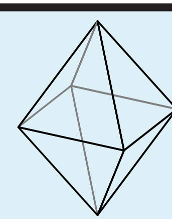

Octahedral (O) **MAS**

$\ell =$	0	1	2	3	4	5	6	7	8	9	10

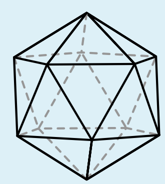

Icosahedral (I)

$\ell =$	0	1	2	3	4	5	6	7	8	9	10

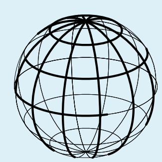

Rotation (SO(3))

$\ell =$	0	1	2	3	4	5	6	7	8	9	10

Averaging of spherical harmonics under selected proper point groups and SO(3). (Adapted by permission of Clarendon Press from A. Samoson, B. Q. Sun, and A. Pines, in *Pulsed Magnetic Resonance: NMR, ESR, and Optics - A recognition of E. L. Hahn.*)

A Solution: Double Rotation

Samoson, Lippmaa, Pines, Mol. Phys., 65, 1023(1988).

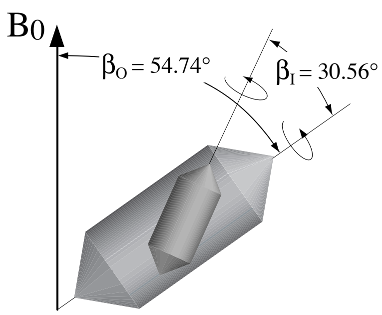

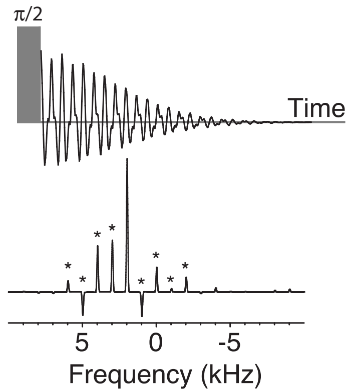

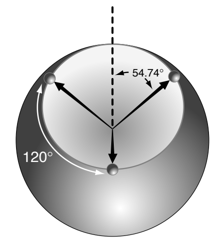

MAS Symmetry

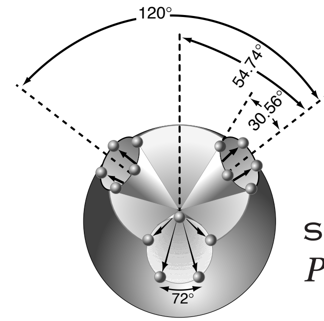

DOR Symmetry

Samoson, Sun, and Pines, *Pulsed Magnetic Resonance: NMR, ESR, and Optics*

^{23}Na DOR of $Na_4P_2O_7$

Engelhardt, Kentgens, Koller, Samoson
Solid State Nuclear Magnetic Resonance **15** 1999, 171–180

Magic Angle Spinning

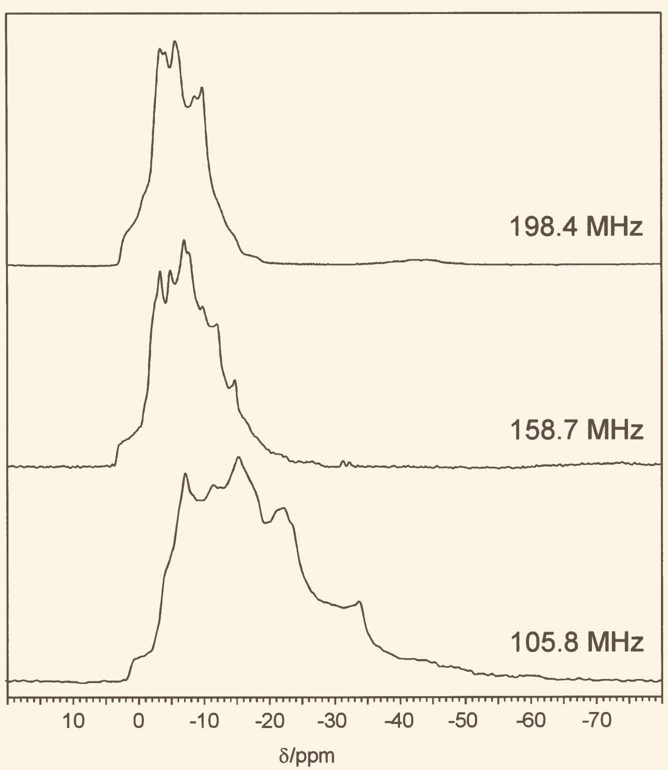

Double Rotation

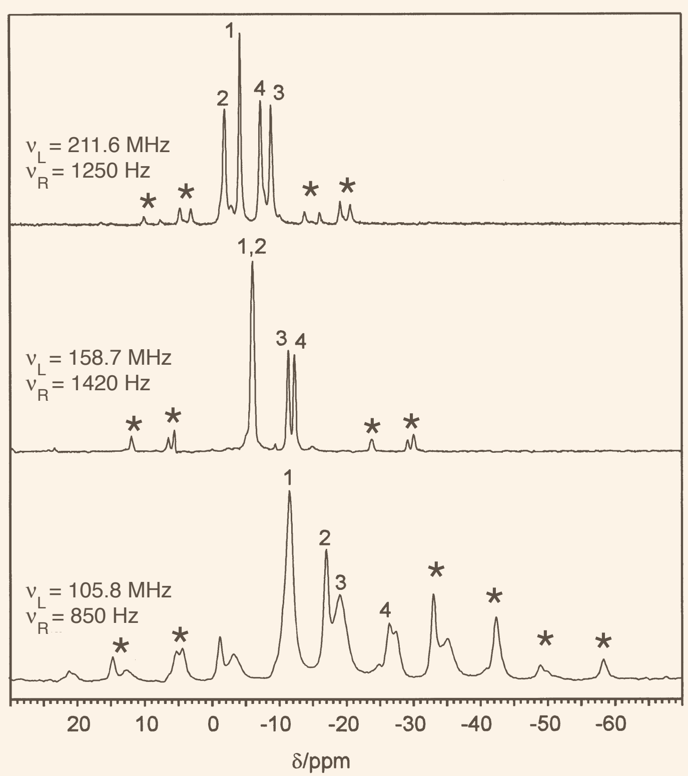

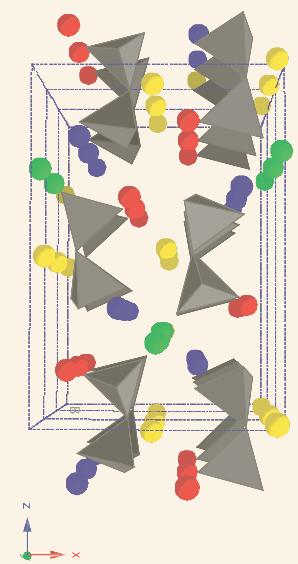

Other Solutions?
Let's make an Echo

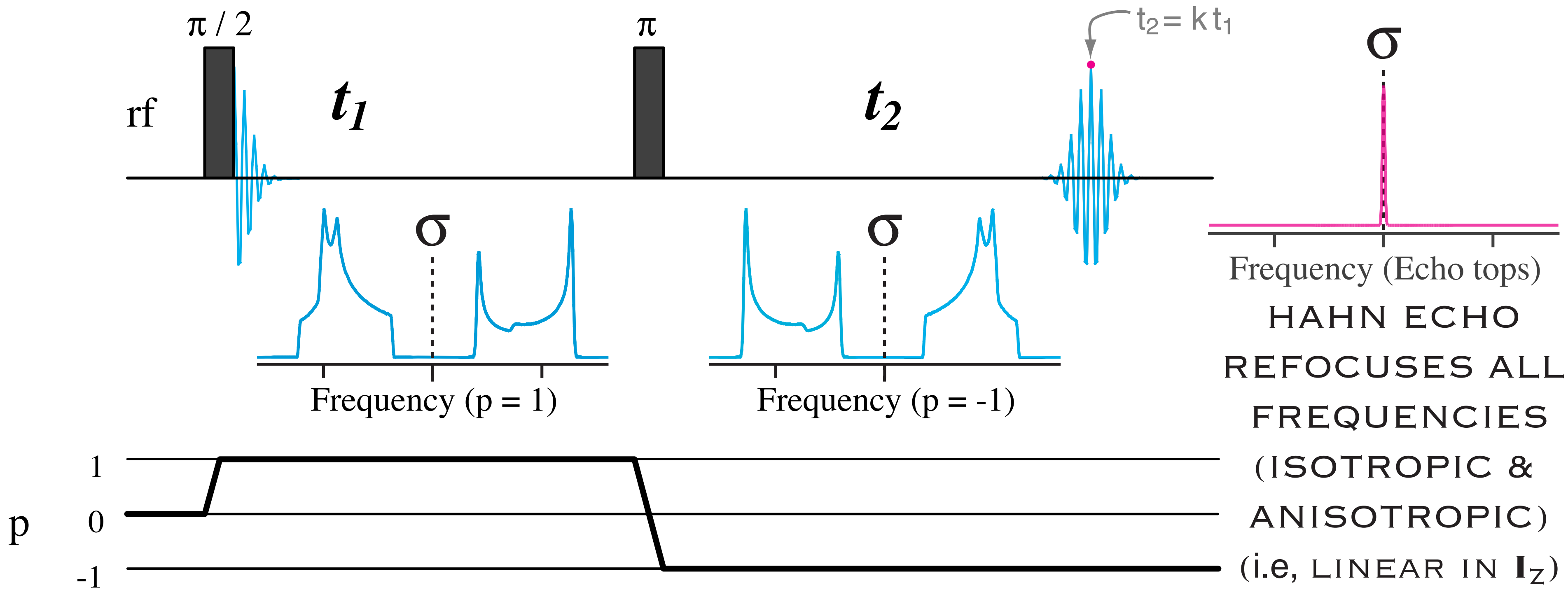

Hahn echo refocuses all frequencies (isotropic & anisotropic) (i.e, linear in $\mathbf{I}_z$)

Find Mirror Image Anisotropic Lineshapes

The key to understanding Dynamic-Angle Spinning

(1988: First High Resolution 2D Method for Quadrupolar Nuclei)

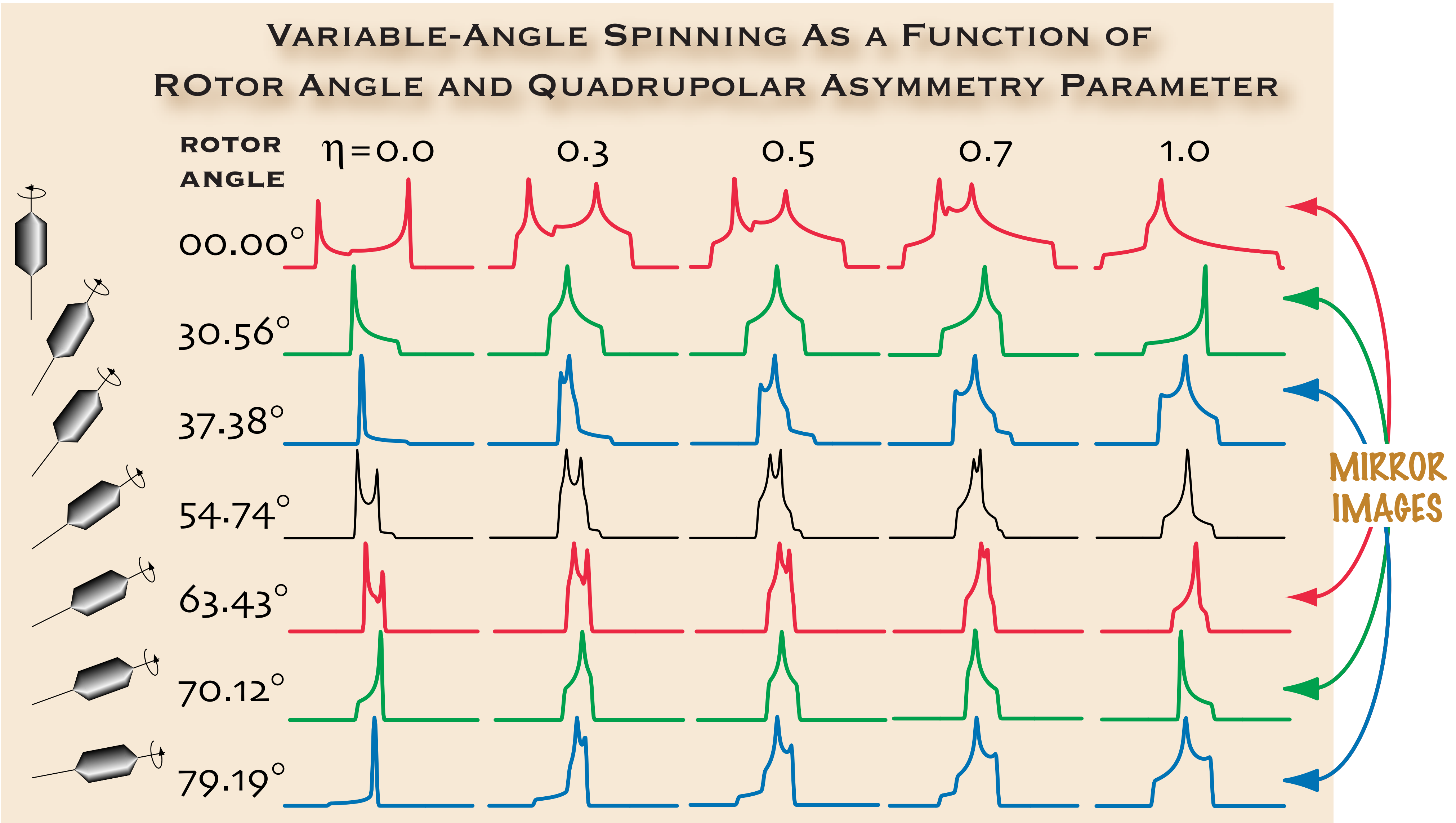

The DAS Echo

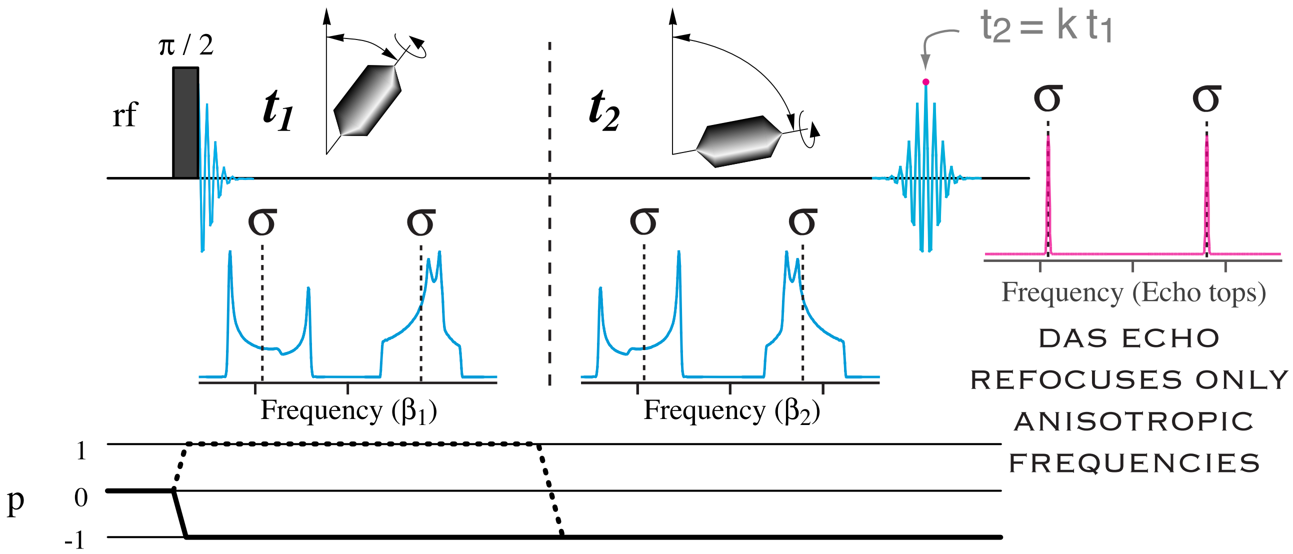

DAS ECHO REFOCUSES ONLY ANISOTROPIC FREQUENCIES

Chmelka et al., ***Nature*, 339,** 42 (1989).
Llor and Virlet, ***Chem. Phys. Lett.*, 152,** 248 (1988).

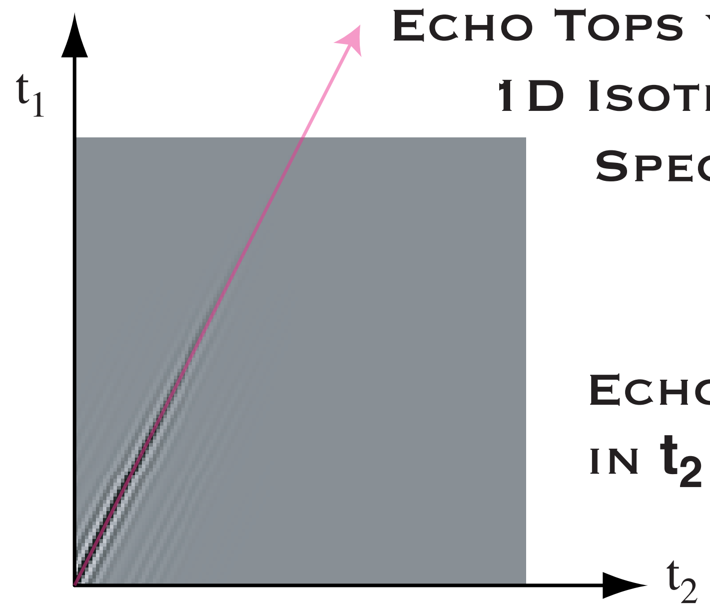

Echo Tops yield 1D Isotropic Spectrum

Echo appears in t_2 at $k\ t_1$.

When does the echo occur in t_2?

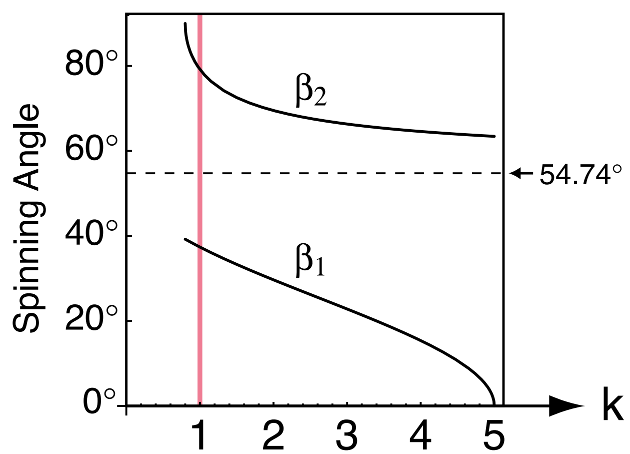

For example, with
$\beta_1 = 37.38°$, $\beta_2 = 79.19°$
we have $k = 1$

2D Dynamic Angle Spinning

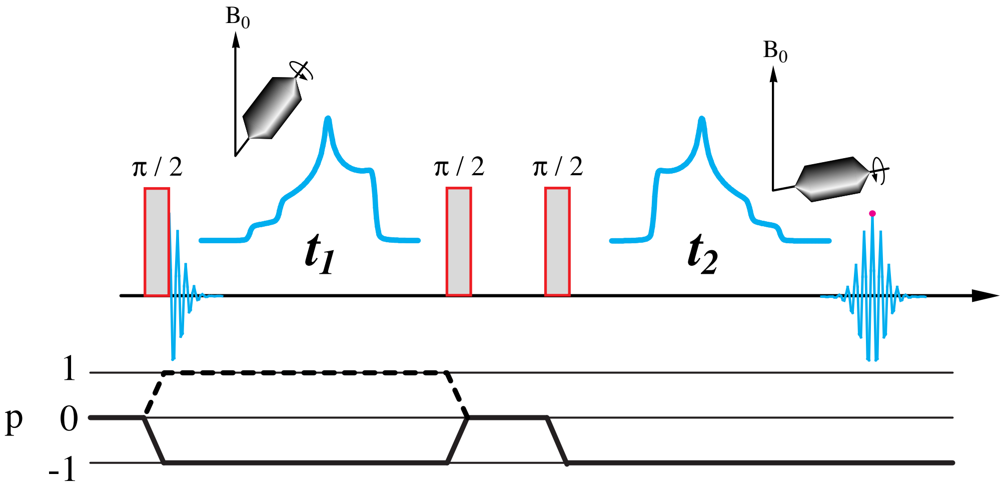

Mueller, Sun, Chingas, Zwanziger, Terao, and Pines, *J. Magn. Reson.*, **86,** 470 (1990).

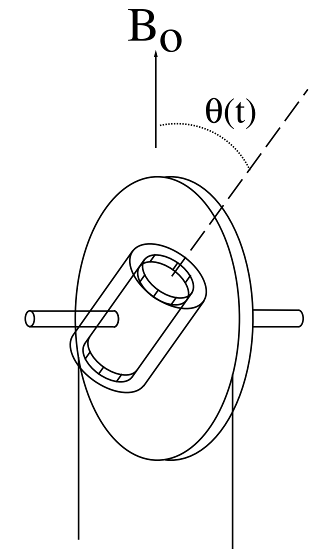

Shifted Echo Acquisition For Pure Absorption Mode 2D Spectra in Solids

J. Magn. Reson. A, **103,** *72-81 (1993).*

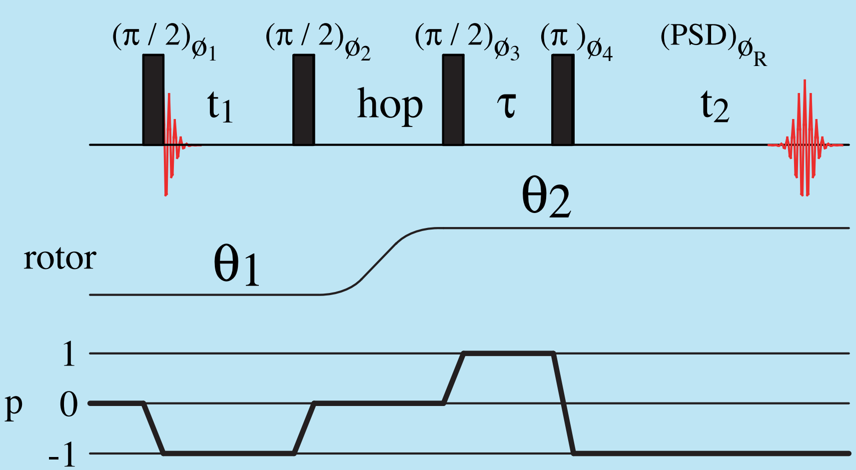

Shearing Transformation

apply t_1 dependent 1st order phase correction to ω_2 dimension

J. Magn. Reson. A, **103,** *72-81 (1993).*

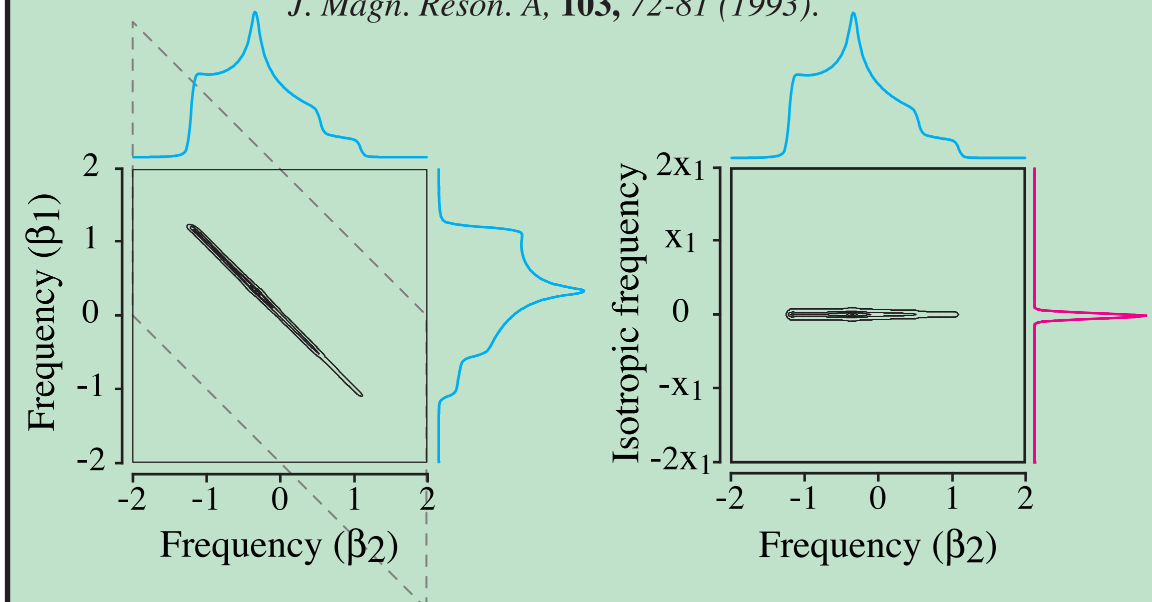

^{17}O 2D DAS of Coesite (A SiO_2 Crystalline Polymorph)

Magic-Angle Spinning

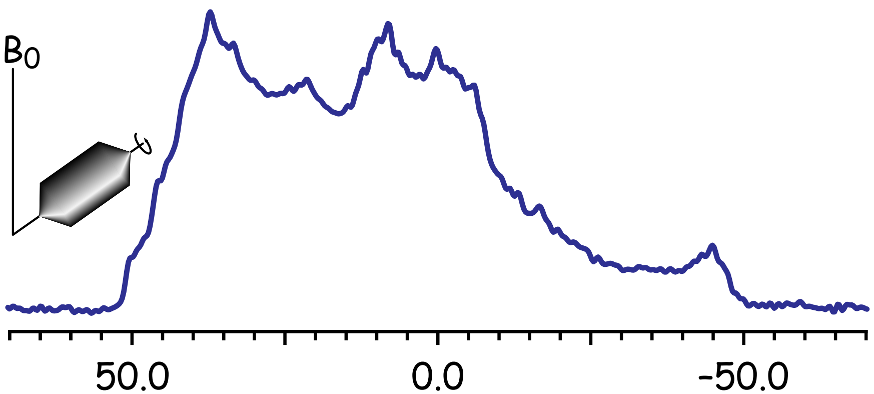

Dynamic-Angle Spinning

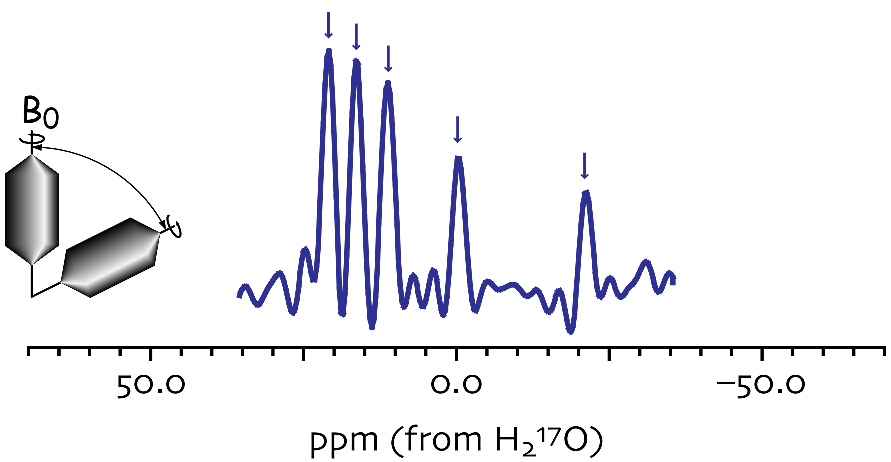

J. Phys. Chem., **99,** 12341 (1995)

Coesite Structural Fragment

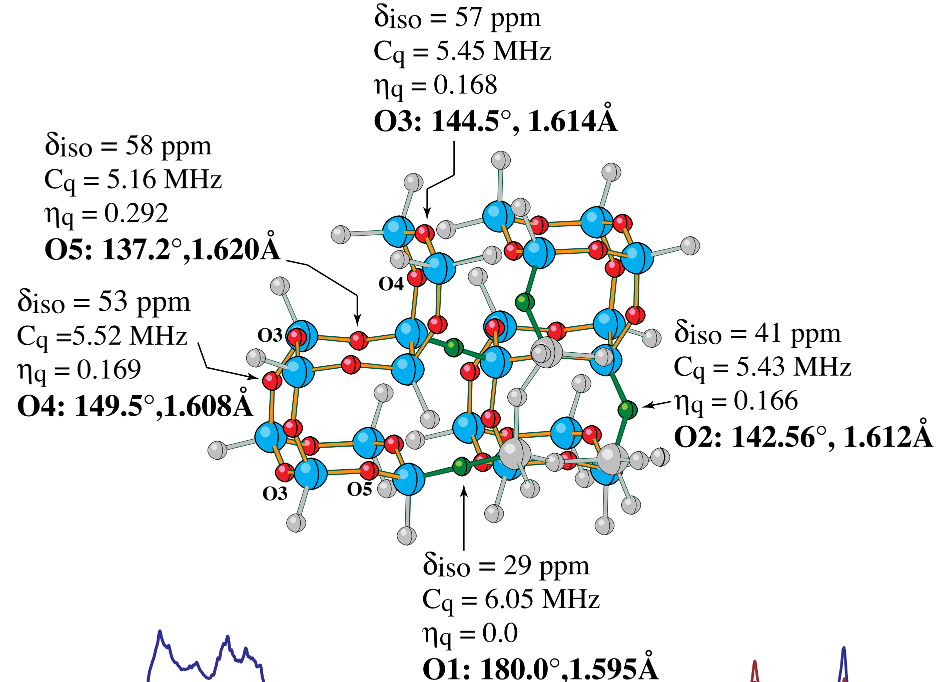

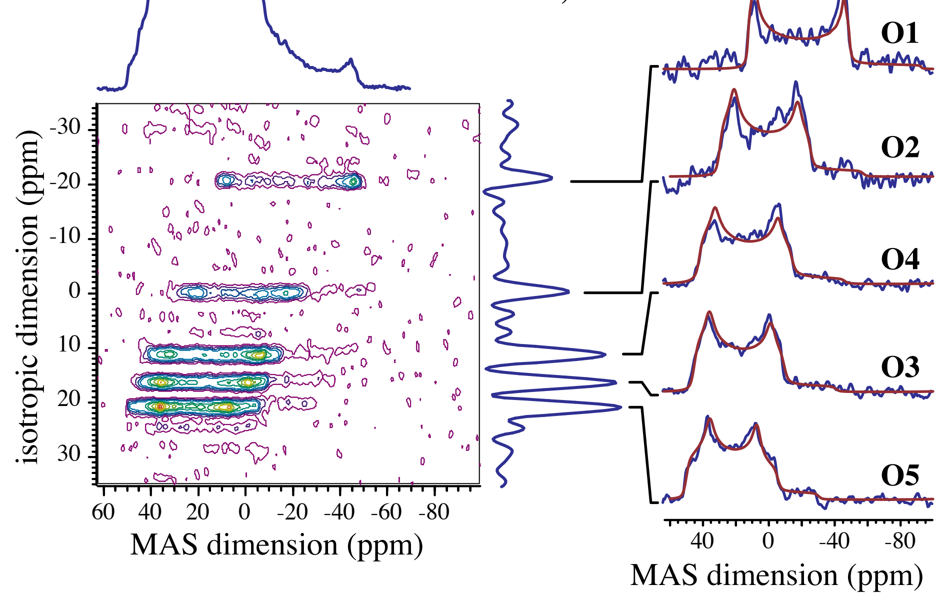

Another Solution: The MQ-MAS Echo (high resolution for The People)

Triple quantum MAS spectrum is the mirror image of the single quantum MAS spectrum

Frydman and Harwood,
J. Am. Chem. Soc., **117,** 5367 (1995)
Medek, Harwood, and Frydman,
J. Am. Chem. Soc. **117,** *12779 (1995)*

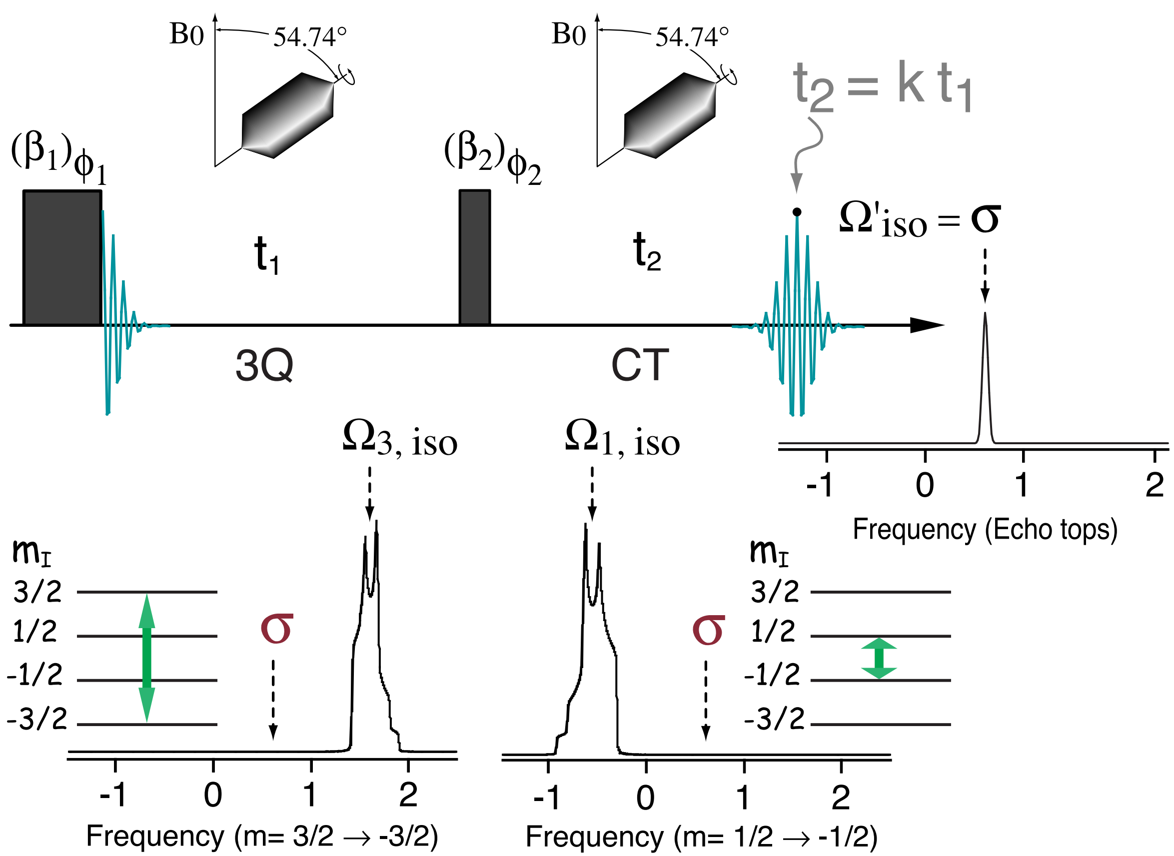

When does the echo occur in t_2?

Spin	t1 transition (m ⟶ -m)	k
3/2:	3QMAS	7/9
5/2:	3QMAS	19/12
	5QMAS	25/12
7/2:	3QMAS	101/45
	5QMAS	11/9
	7QMAS	161/45
9/2:	3QMAS	91/36
	5QMAS	95/36
	7QMAS	7/18
	9QMAS	31/6

2D Shifted-Echo MQ-MAS

Massiot et al., *SSNMR,* **6,** 73 (1996)

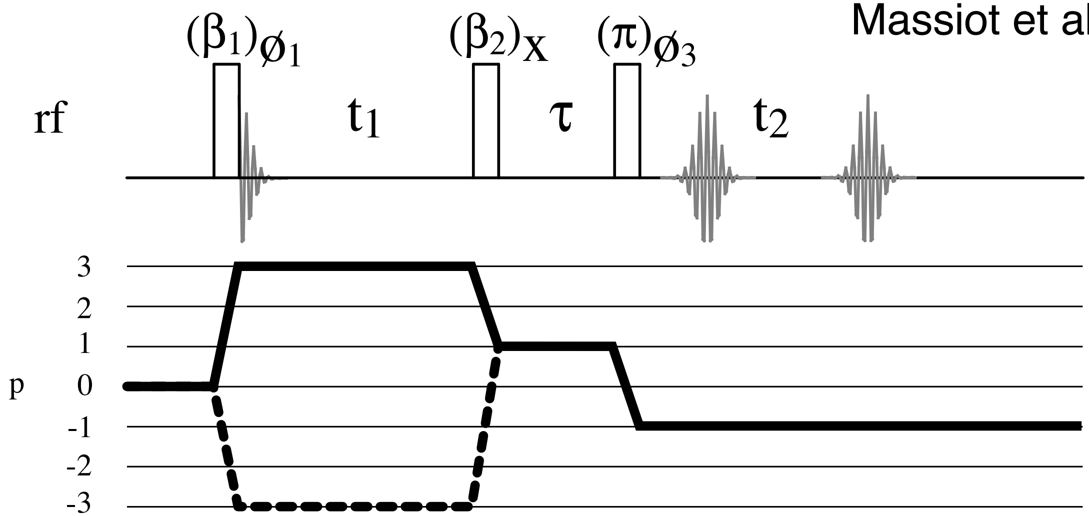

After Shearing Transformation:

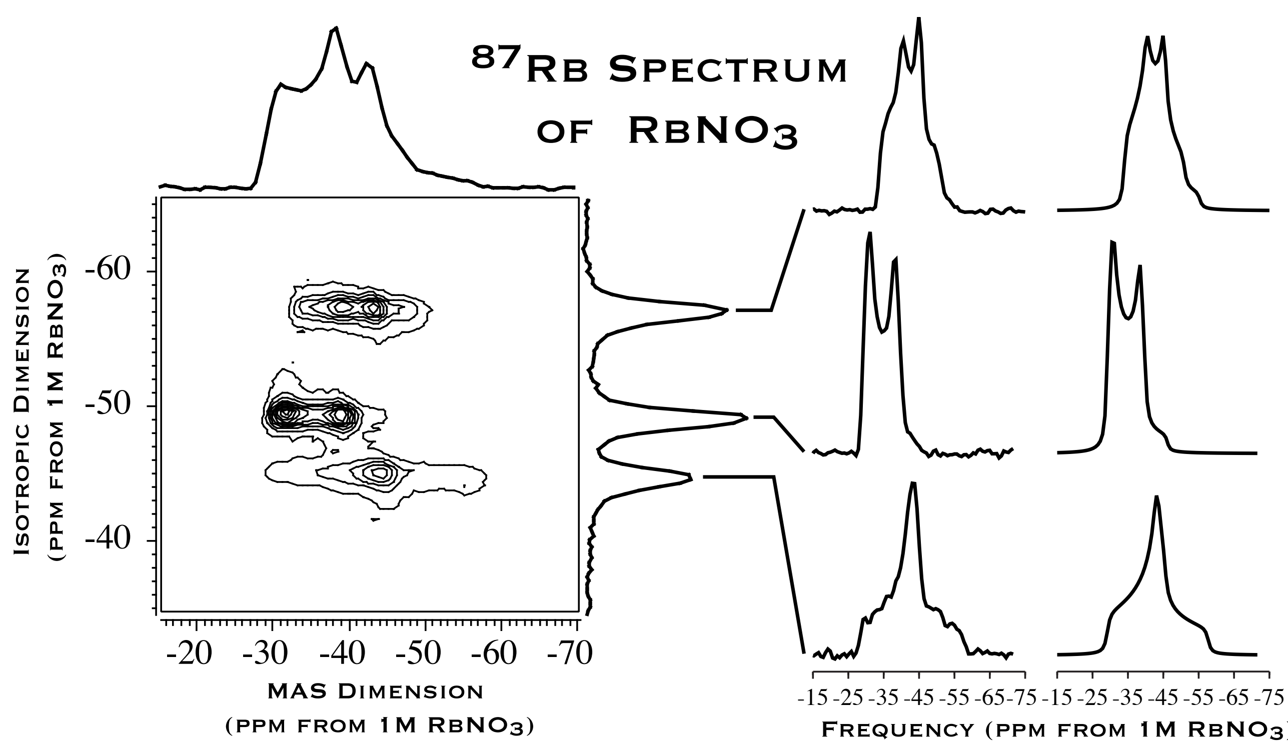

...and Another Solution: The ST-MAS Echo

Z. Gan, *J. Am. Chem. Soc.* 2000, **122,** 3242-3243

The satellite transition MAS spectrum is the mirror image of the central transition MAS spectrum

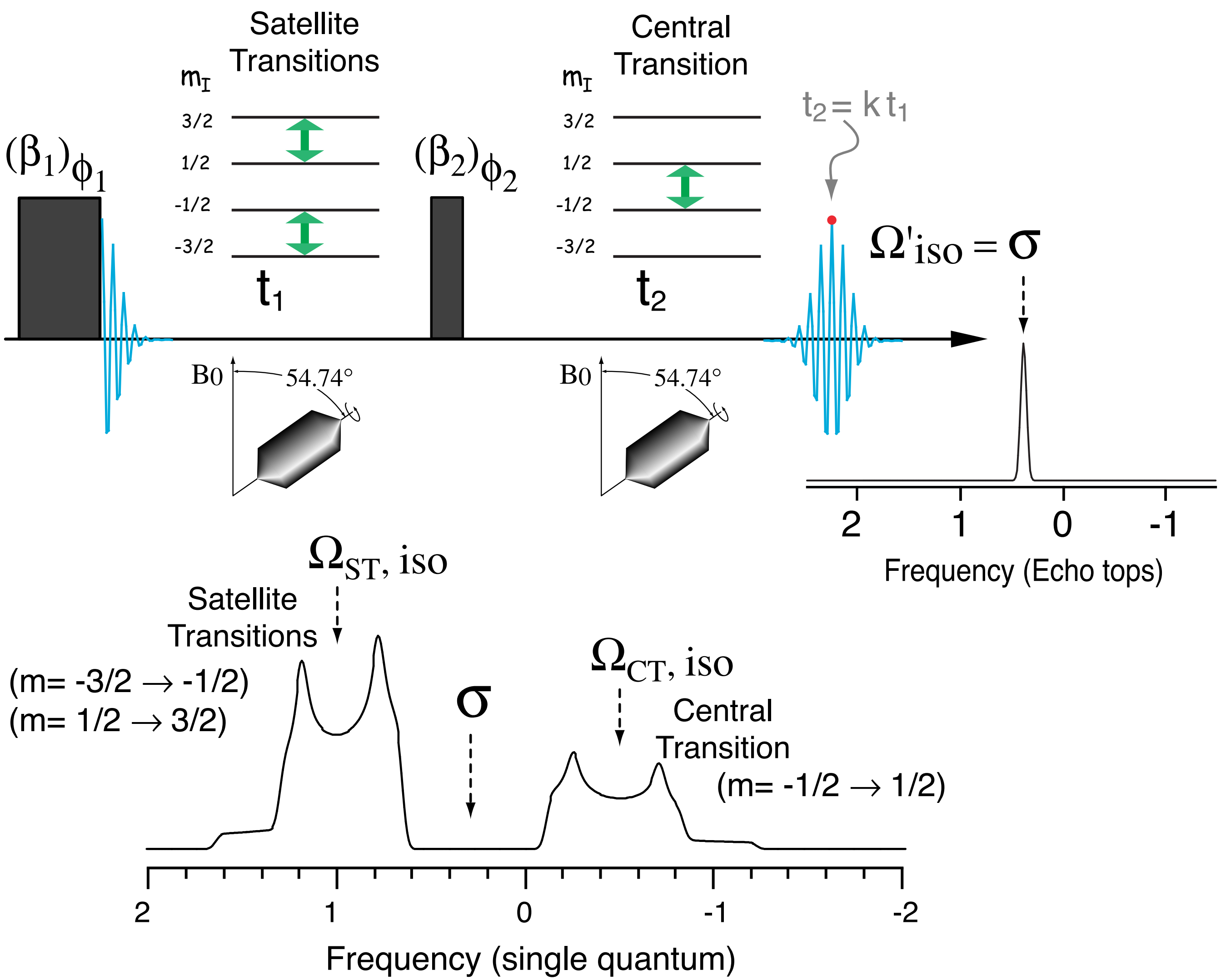

When does the echo occur in t_2?

Spin	t_1 transition	k
3/2:	1st satellites	8/9
5/2:	1st satellites	7/24
	2nd satellites	11/6
7/2:	1st satellites	28/45
	2nd satellites	23/45
	3rd satellites	12/5
9/2:	1st satellites	55/72
	2nd satellites	1/18
	3rd satellites	9/8
	4th satellites	25/9

Use Double Quantum Filtered ST-MAS to eliminate undesired CT-CT correlation

Hyung-Tae Kwak and Zhehong Gan, *J. Magn. Reson.* **164** (2003) 369–372

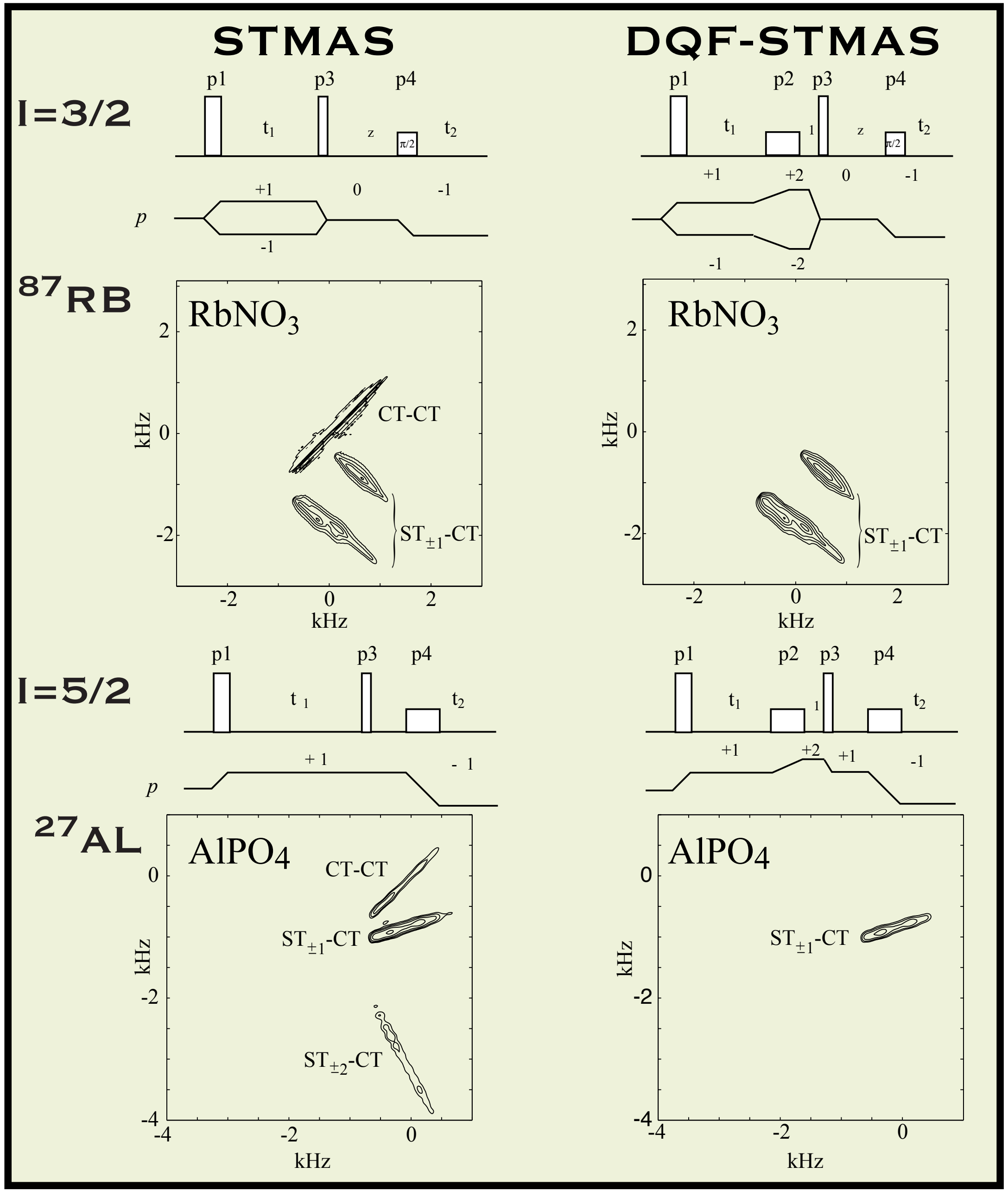

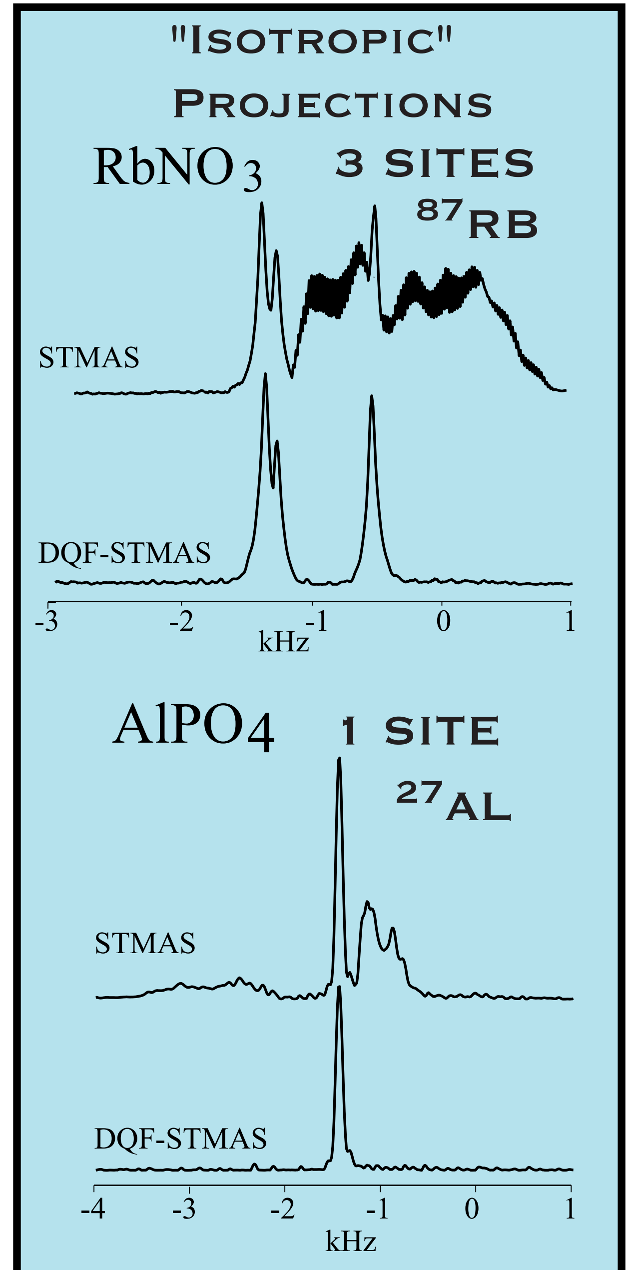

	Advantages	Disadvantages
DOR:	• Quantitative • High Sensitivity • Low rf power • One dimensional experiment - Quick experiment (In principle)	• Special Probe Required • Stable spinning requires finesse • Slow spinning speeds - (large # of sidebands) • Large coil ... low rf power - poor decoupling.
DAS:	• Quantitative • High Sensitivity, even with nuclei having large quad. couplings • Low rf power • works well for dilute quadrupolar nuclei	• Special Probe Required • Fails in presence of strong homonuclear dipolar couplings • long hop times (30 ms) limits use to samples with long longitudinal relaxation.
MQ-MAS:	• Easiest to implement (no special probe) • Works well for Abundant nuclei • Works well for nuclei with short longitudinal relaxation	• Not always quantitative • requires high rf power for excitation and mixing • Poor sensitivity for large Cq • Complex spinning sideband behavior
ST-MAS:	• Easy to implement (no special probe) • excites only single quantum transitions • Works well for Abundant nuclei • Works well for nuclei with short longitudinal relaxation	• Sensitive to magic-angle misset ($< 0.01^\circ$) • stable spinning speed required. • requires high rf power for satellite excitation. • Poor sensitivity for large Cq • Not always quantitative • Complex spinning sideband behavior • fails to remove 3rd and other higher-order effects • Fails when there's motional averaging of satellite lineshapes.

A Few Loose Ends...

Field Dependance of Isotropic Shift

Isotropic frequency of quadrupolar nucleus is sum of isotropic
(1) chemical shift and
(2) 2nd order quadrupolar shift.

$$\Omega^{(iso)} = \delta_{iso}^{(CS)}(\text{ppm}) - \frac{1}{40}\frac{P_q^2}{\nu_0^2} \times 10^6\ (\text{ppm})$$

$$P_q = C_Q(1+\eta^2/3)^{1/2}$$

^{87}Rb DAS Spectra of $RbNO_3$

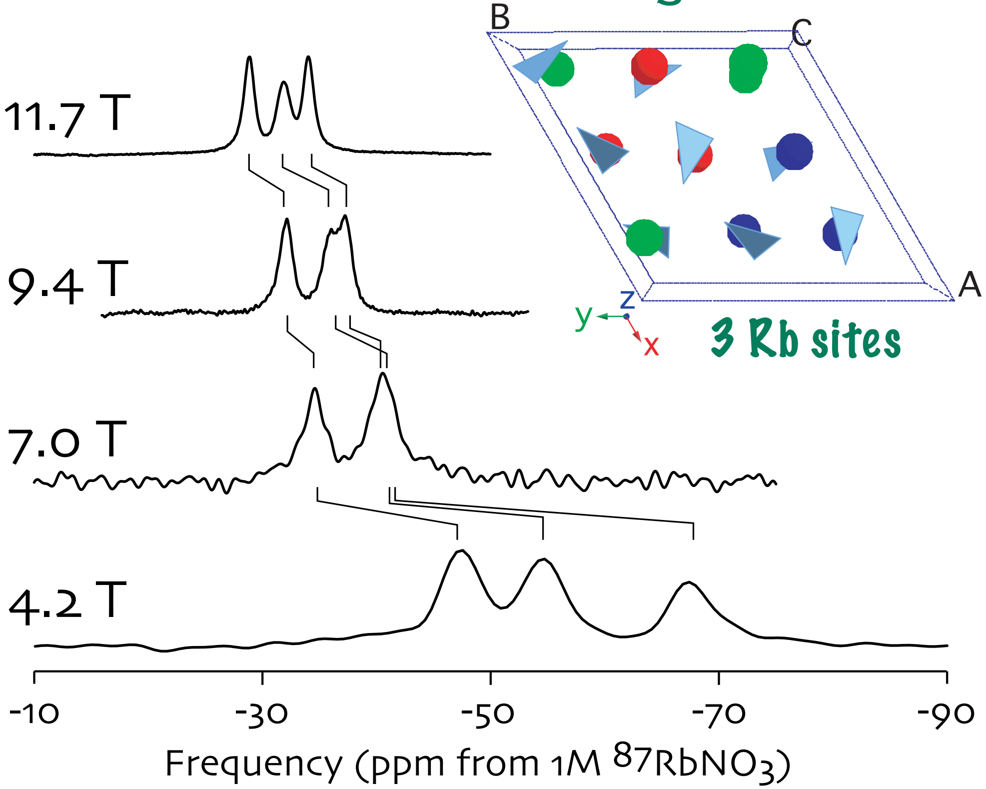

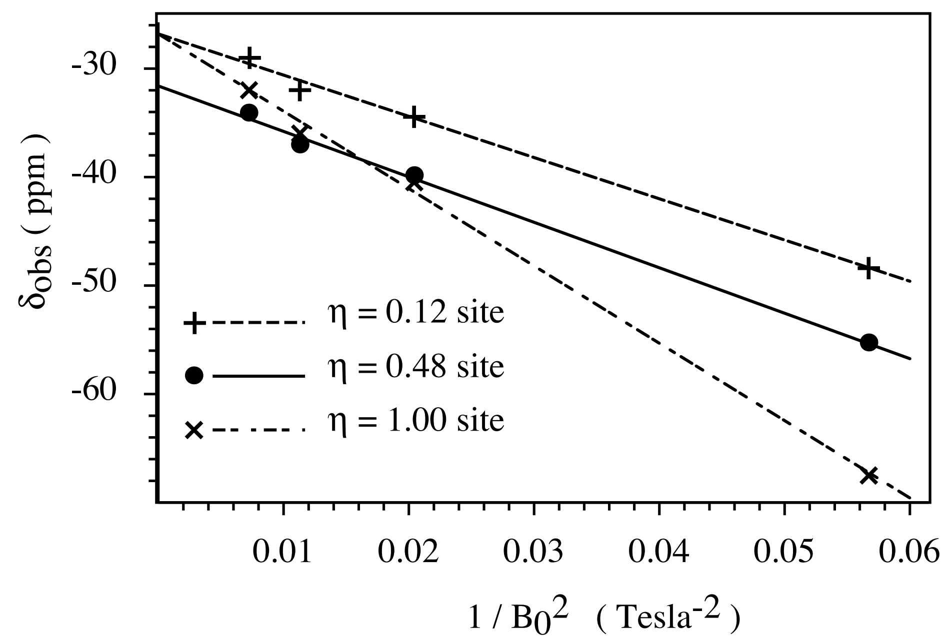

Baltisberger, Gann, Wooten, Chang, Mueller, and Pines, *J. Am. Chem. Soc.*, 1992, **114**, 7489

Warning: Never label spectrum axis of quadrupolar nuclei in Solids as "Chemical Shift". Only true in limit that P_Q/ν_0 goes to zero.

The Fourier Transform, Shift Theorem, and Shearing Transformations

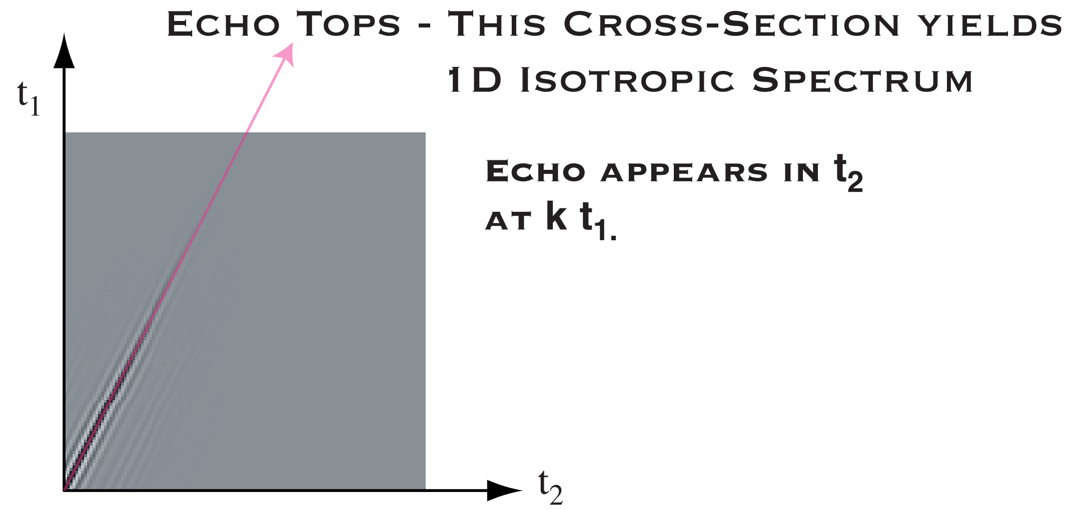

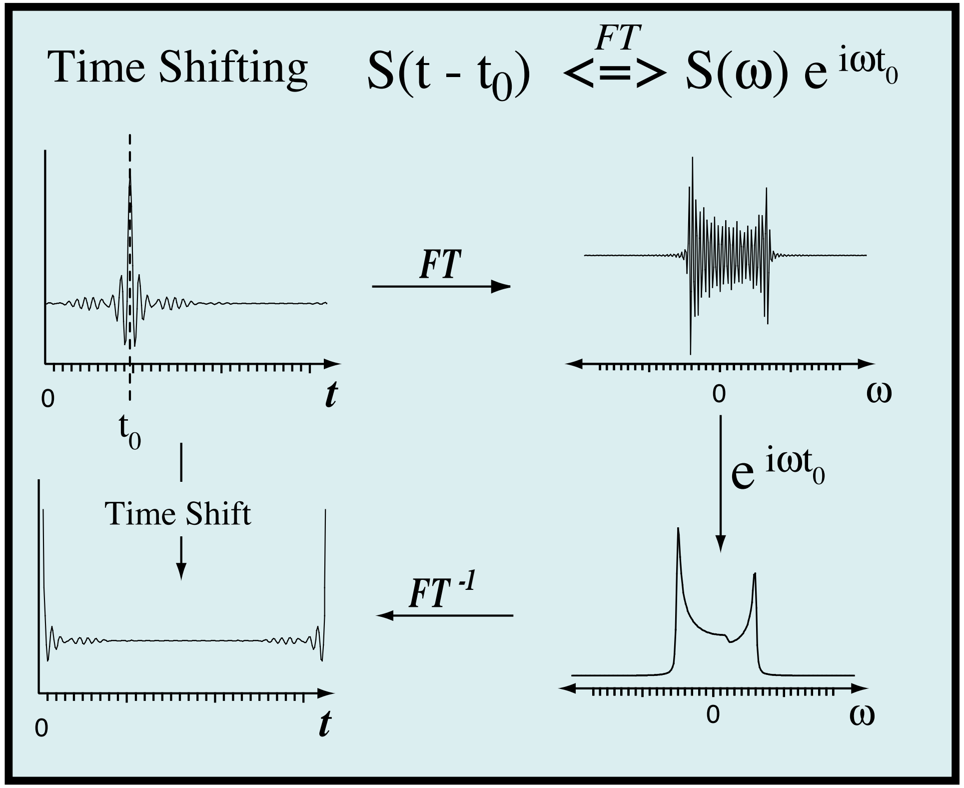

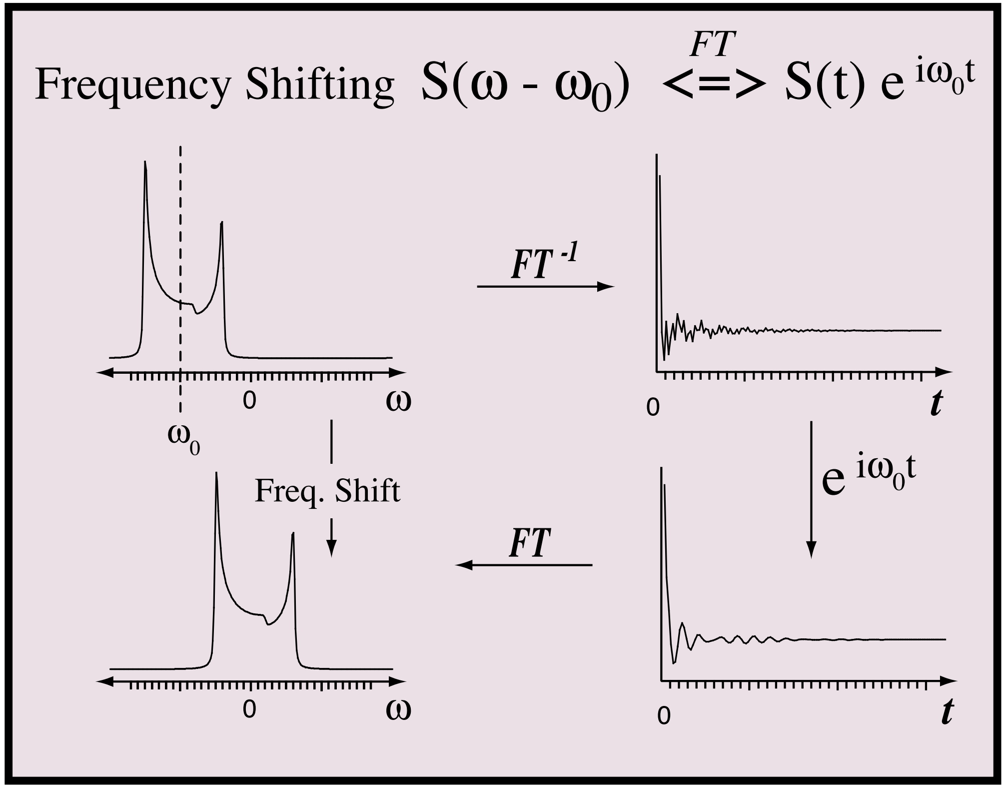

Shearing Transformation in DAS, MQ-MAS, ST-MAS

J. Magn. Reson. A, **103,** 72-81 (1993).
J. Magn. Reson. A, **102,** 195-204 (1993).

$$\mathbf{t}' = \mathbf{A}\mathbf{t}, \quad \text{where} \quad s'(\mathbf{t}) = s(\mathbf{A}\mathbf{t})$$

$$\mathbf{A} = \begin{pmatrix} 1+k & 0 \\ -k & 1 \end{pmatrix}$$

$$\tilde{\omega}' = \tilde{\omega}\mathbf{A}^{-1},$$

$$\text{where} \quad S'(\tilde{\omega}) = \frac{1}{|\mathbf{A}|} S(\tilde{\omega}\mathbf{A}^{-1})$$

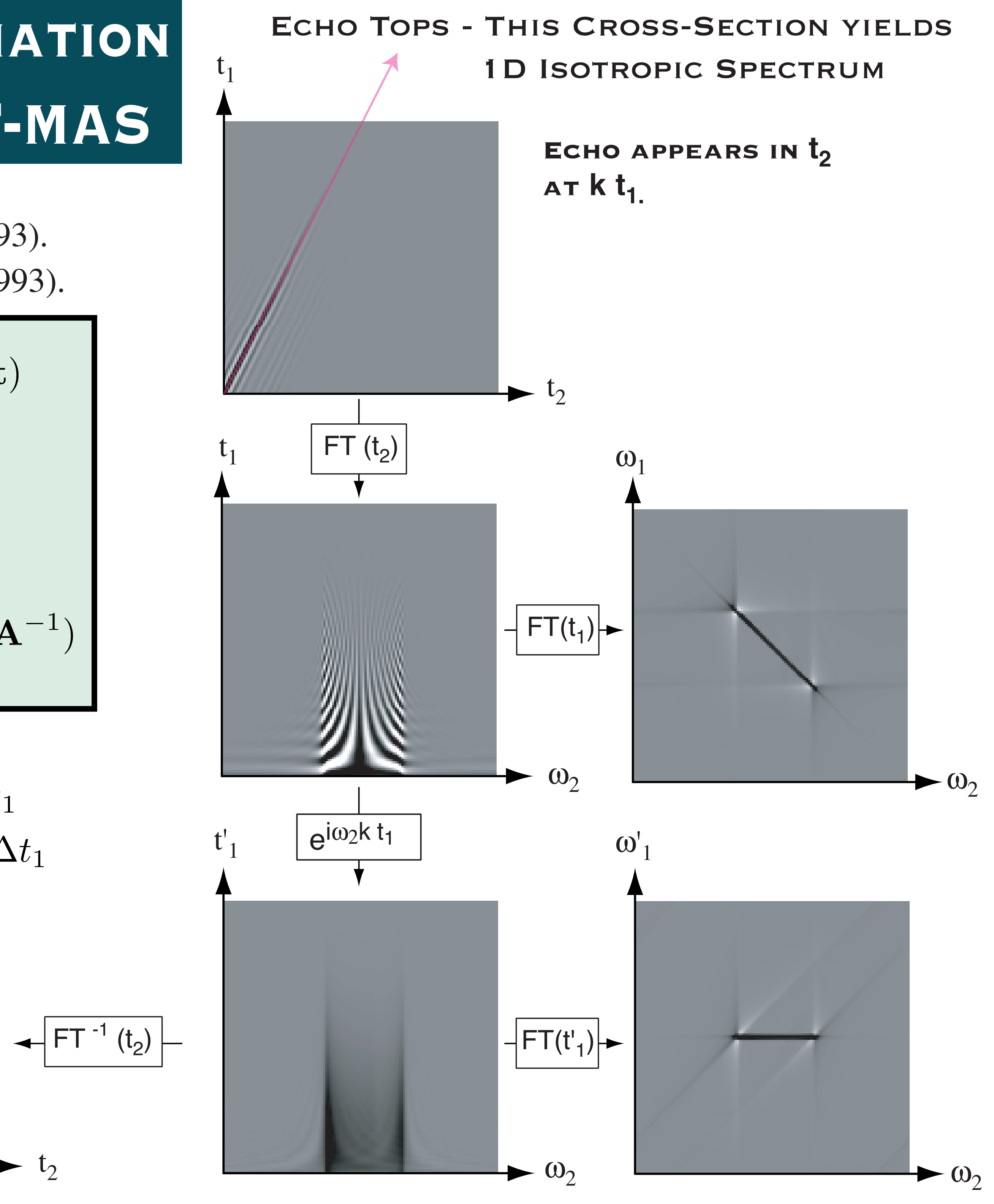

$$t'_1 = (1+k)t_1$$
$$\Delta t'_1 = (1+k)\Delta t_1$$

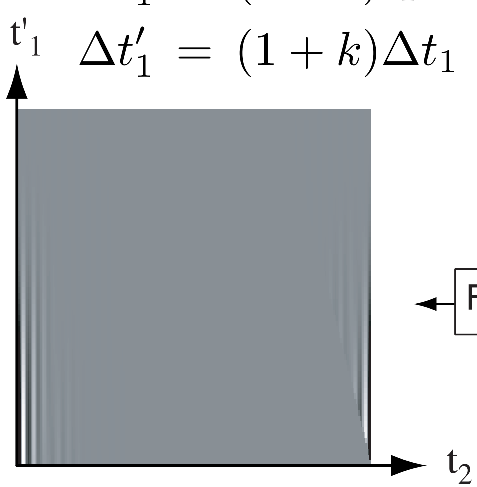

Effect of Shearing Transformation on Spinning Sidebands Positions

Unsheared Spectrum

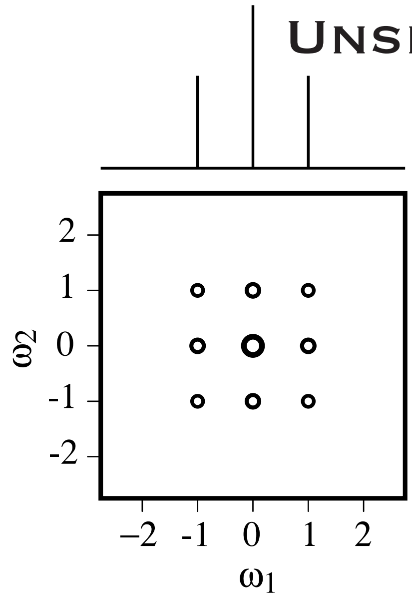

Projection contains sidebands at integer multiples of rotor frequency

J. Magn. Reson. A, 102, 195-204 (1993)

Sheared Spectra

Projection contains sidebands at sum/difference of non-integer multiples of rotor frequency

K = 1

Sidebands appear at 0.5 ω_R

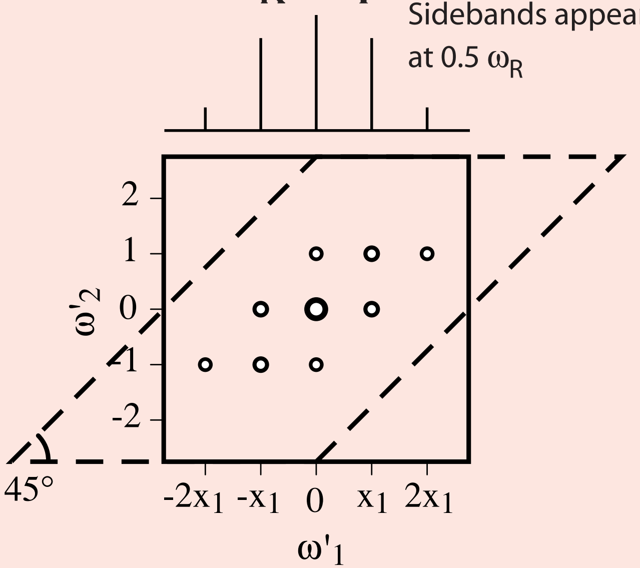

Shear angle 45°

K = 1.273

Sidebands appear at sum and difference of 0.44 ω_R and 0.56 ω_R

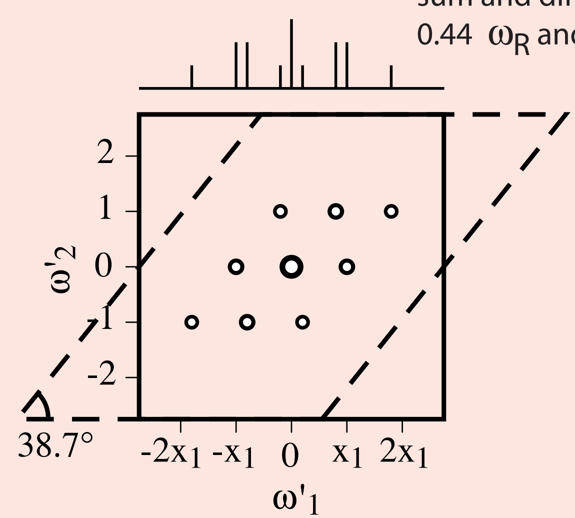

Shear angle 38.7°

Hypercomplex Processing of DAS, MQ-MAS, ST-MAS

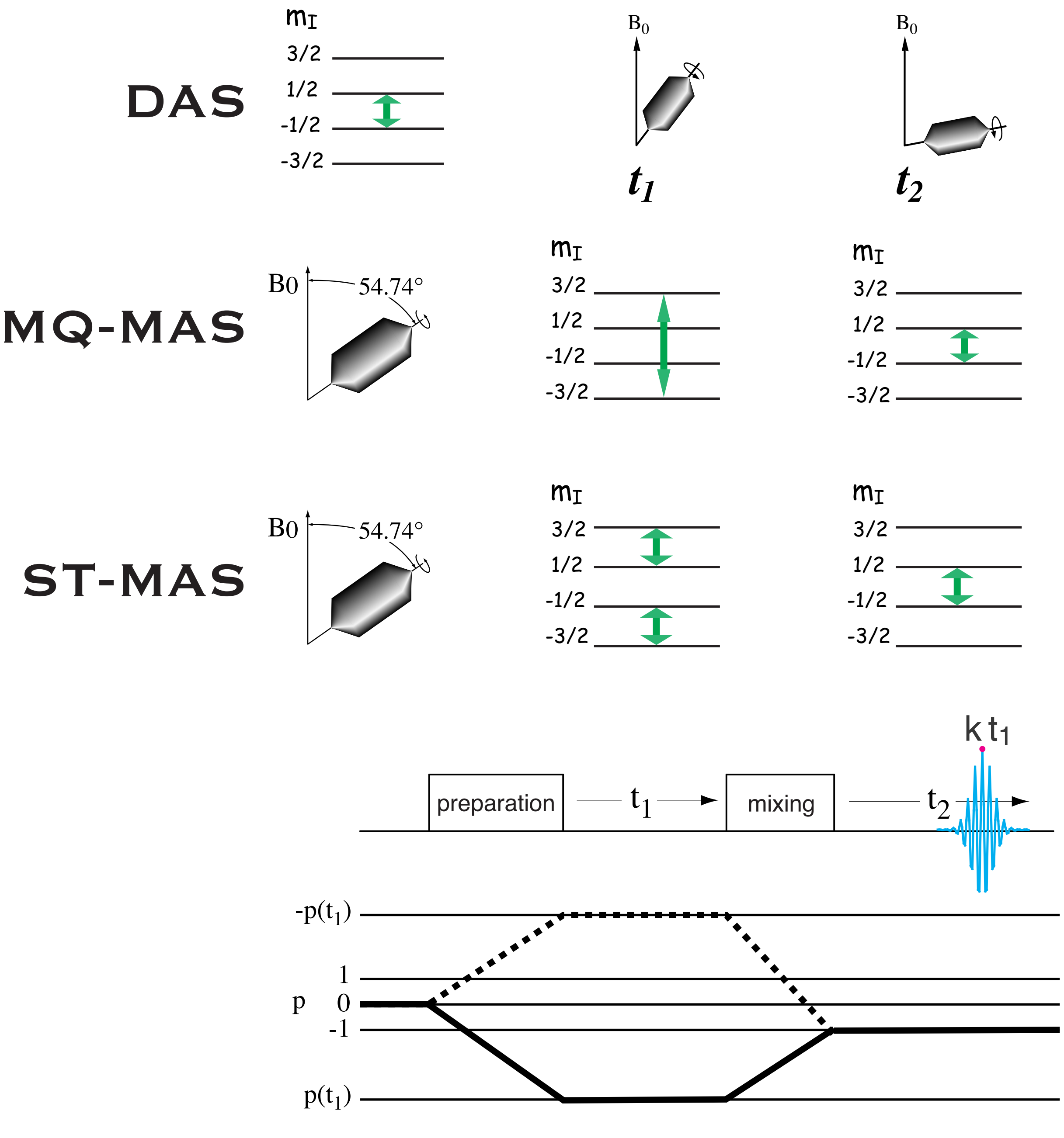

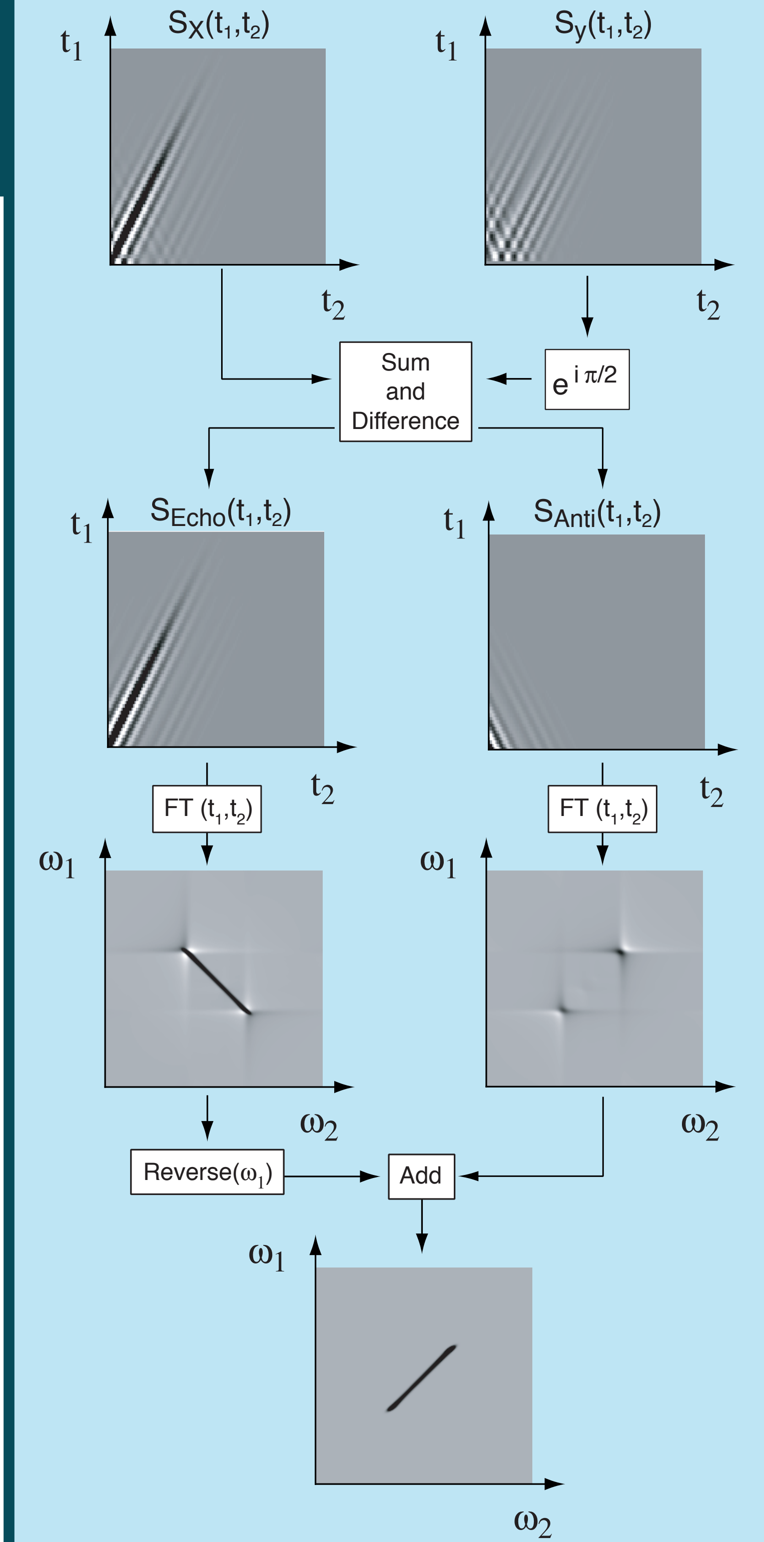

Shifted Echo Data Acquisition and Processing of DAS, MQ-MAS, ST-MAS

J. Magn. Reson. A, **103,** 72-81 (1993).

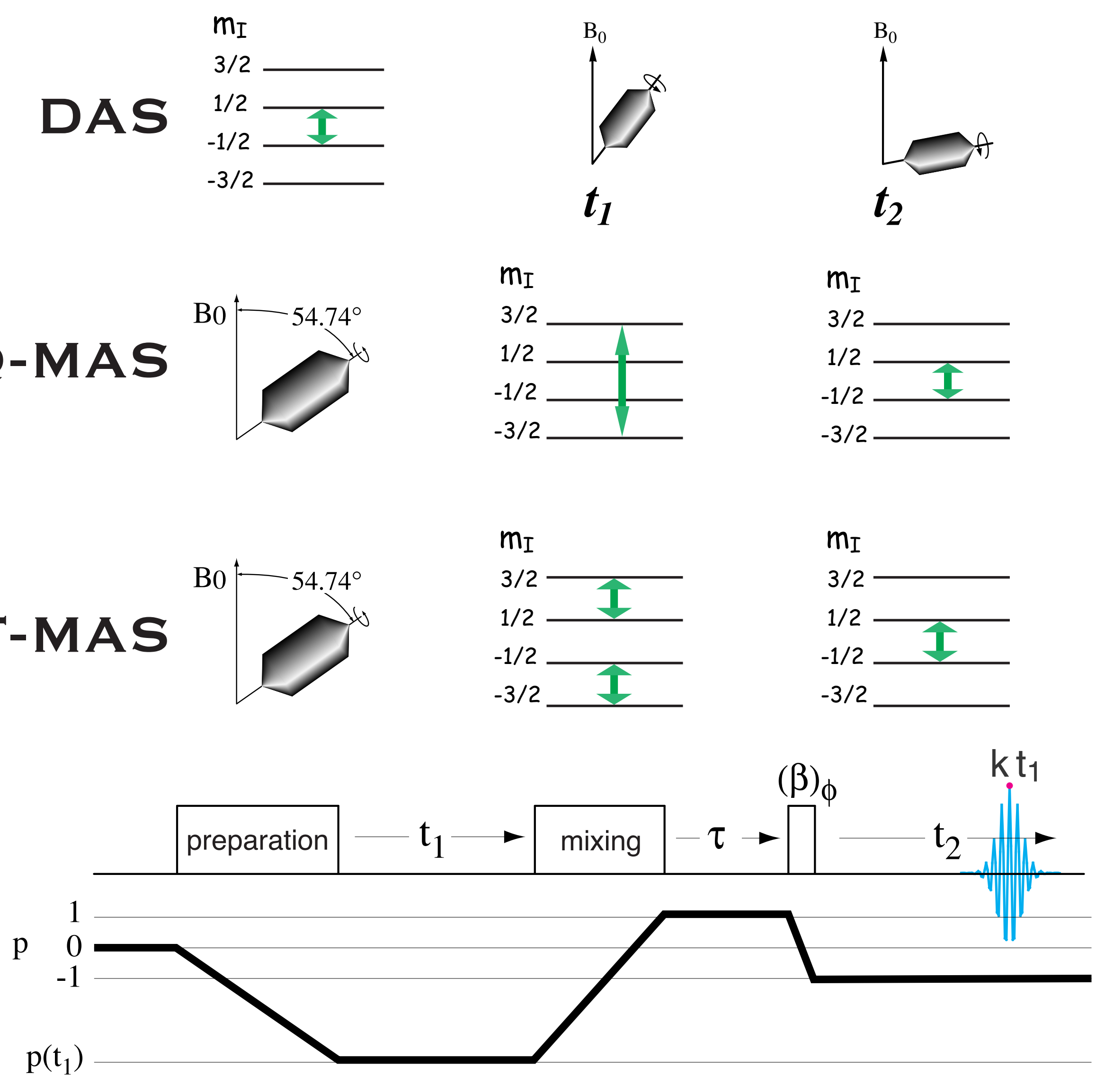

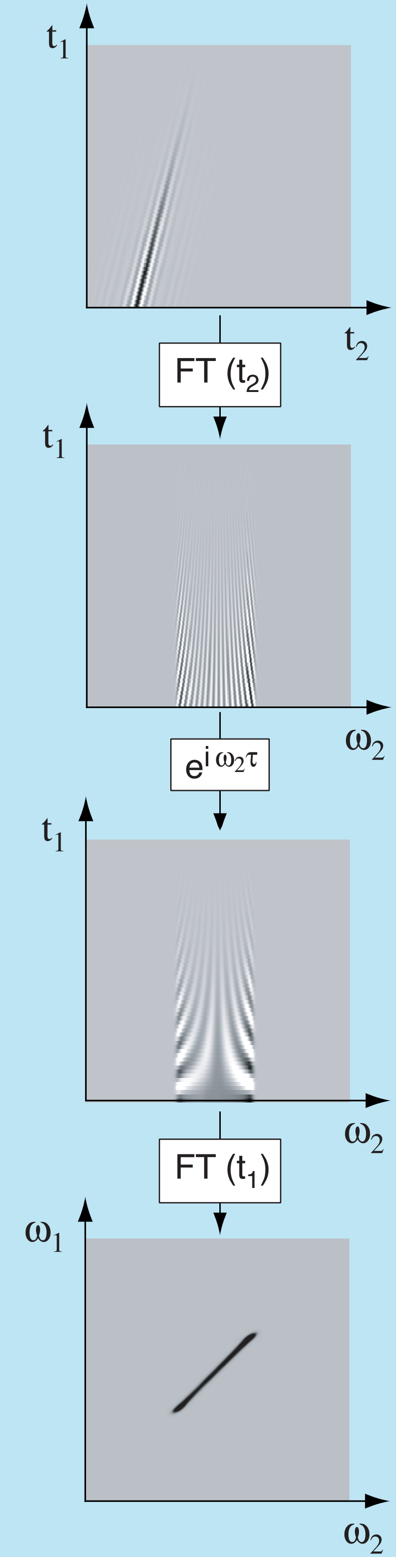

Pay the Bills...

Interpreting Quadrupolar Couplings (Electric Field Gradients)

$$H_q = \sum_k (-1)^k \underbrace{R_{2k}(\Omega_q)}_{\text{Electric Field Gradient at the Nucleus}} \underbrace{\left[\sqrt{\frac{3}{2}}\frac{eQ_{\gamma I}}{I(2I-1)}T_{2-k}\right]}_{\text{Nuclear Quadrupole Moment}}$$

Electric Field Gradient at the Nucleus

$$R_{2,k} = \sum_{\text{all electrons}} E_{2,k}(e) + \sum_{\text{all nuclei}} N_{2,k}(n)$$

Surrounding Electrons

$$E_{2,k}(e) = -e\sqrt{\frac{4\pi}{5}}\frac{1}{r_e^3}Y_{2,k}(\theta_e,\phi_e)$$

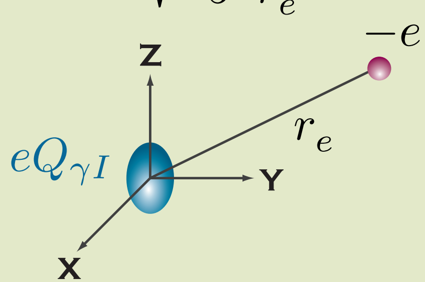

Surrounding Nuclei

$$N_{2,k}(n) = Z_n e\sqrt{\frac{4\pi}{5}}\frac{1}{r_n^3}Y_{2,k}(\theta_n,\phi_n)$$

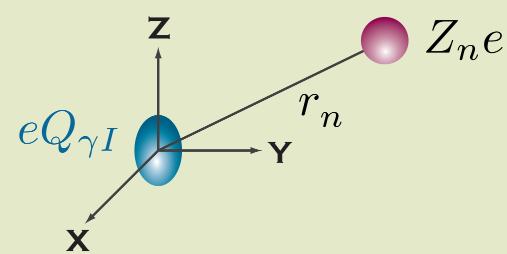

Total Electric Field Gradient at the Nucleus

$$\langle R_{2,k}\rangle = \langle \Psi | R_{2,k} | \Psi \rangle$$

Complete nuclear and electronic wavefunction

The Electric Field Gradient Tensor and its orientation

- EFG is 2nd rank traceless tensor: 5 elements, $\langle R_{2,k} \rangle$, with k = -2,-1,0,1,2.
- There exists a principal axis coordinate system (PAS) where tensor is diagonal... $\langle R^{\mathrm{PAS}}_{2,\pm1} \rangle = 0$
- Further define PAS such that $|\langle R^{\mathrm{PAS}}_{2,0} \rangle| > |\langle R^{\mathrm{PAS}}_{2,\pm2} \rangle|$

...labeling PAS components as $\langle \rho_{2,k} \rangle \equiv \langle R^{\mathrm{PAS}}_{2,k} \rangle$

For example, in a C-D bond the ^{2}D EFG PAS is directed along the C-D bond axis.

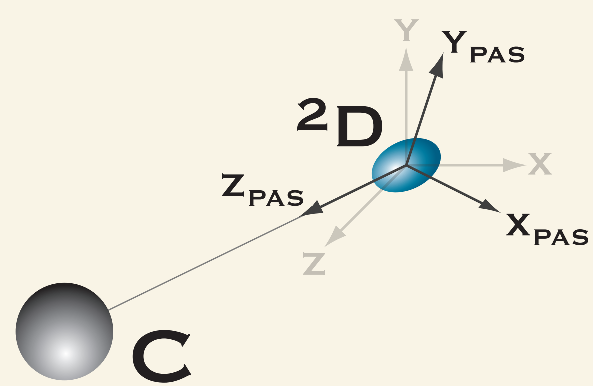

- Quadrupolar coupling Constant and Asymmetry parameters are defined ...

$$C_q = 2\,\frac{eQ}{h}\langle \rho_{2,0} \rangle \quad \text{and} \quad \eta_q C_q = 2\sqrt{6}\,\frac{eQ}{h}\langle \rho_{2,\pm2} \rangle$$

In Cartesian Coordinates... $C_q = e^2 Q \langle q_{zz} \rangle / h, \quad \text{and} \quad \eta_q = \dfrac{\langle q_{xx} \rangle - \langle q_{yy} \rangle}{\langle q_{zz} \rangle}$

Note that... $\langle q_{zz} \rangle + \langle q_{yy} \rangle + \langle q_{xx} \rangle = 0$

Point Charge Model for Predicting Electric Field Gradients

- No analytical expression for EFG exists without approximations.
- Most drastic is the Point Charge Model: It's crude, but often provides a qualtitative understanding, and with calibration can sometimes be quantitative.

$$\langle R_{2,k} \rangle = \sum_{j=1}^{n} \frac{Z_j e}{d_i^3} \sqrt{\frac{4\pi}{5}} Y_{2,k}(\theta_j, \phi_j)$$

Approximate coordinating atoms as point charges and calculate sum of all coordinating atoms.

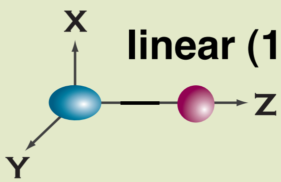

linear (1-coord.) $\theta = 0, \phi = 0$

$$\langle R_{2,0} \rangle = \frac{Ze}{d^3}, \quad \langle R_{2,\pm 1} \rangle = 0, \text{ and } \langle R_{2,\pm 2} \rangle = 0$$

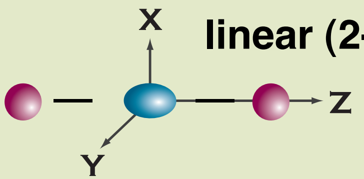

linear (2-coord.) $\theta_1 = 0, \quad \phi_1 = 0$

$\theta_2 = 180^\circ, \phi_2 = 0$

$$\langle R_{2,0} \rangle = 2\frac{Ze}{d^3}, \langle R_{2,\pm 1} \rangle = 0, \text{ and } \langle R_{2,\pm 2} \rangle = 0$$

Point Charge model predicts Cq doubles, and PAS unchanged when atom goes from one to two-coordinated linear.

Experimental ^{17}O NMR measurements in Silicates

Non-Bridging Oxygen Si-^{17}O$^-$

α-$Na_2Si_2O_5$ C_Q = 2.40 MHz, η = 0.20

$Li_2Si_2O_5$ C_Q = 2.45 MHz, η = 0.10

Bridging Oxygen Si-^{17}O-Si

α-$Na_2Si_2O_5$ C_Q = 5.74 MHz, η = 0.20

$Li_2Si_2O_5$ C_Q = 5.60 MHz, η = 0.10

Maekawa, Florian, Massiot, Kiyono, Nakamura, *J. Phys. Chem.* 1996, **100** (17), 5525-5532.

Xue, Stebbins, Kanzaki, *Am. Miner.* 1994, **79,** 31.

Point Charge Model for Predicting Electric Field Gradients

Trigonal Planar

Place quadrupole nucleus at the origin and the z-axis perpendicular to the plane containing 3 point charges

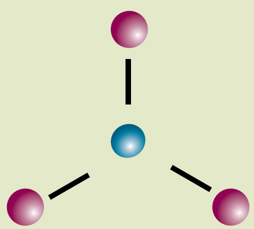

$$\theta = 90^\circ, \phi = 0, \pm 120^\circ$$

$$\langle R_{2,0} \rangle = -\frac{3}{2}\frac{Ze}{d^3}, \qquad \langle R_{2,\pm 1} \rangle = 0, \quad \text{and} \quad \langle R_{2,\pm 2} \rangle = 0$$

- z-axis of efg PAS is perpendicular to plane containing nucleus and coordinating charges.
- Asymmetry parameter is zero, and sign of the quadrupole coupling constant is opposite to linear cases.

Tetrahedral

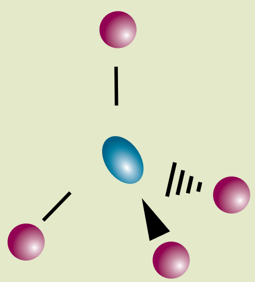

$$\langle R_{2,0} \rangle = 0, \quad \langle R_{2,\pm 1} \rangle = 0, \quad \text{and} \quad \langle R_{2,\pm 2} \rangle = 0$$

^{11}B Examples from Borosilicates...

	Cq	eta
Trigonal Planar $^{11}BO_3$ (ring)	2.65 MHz	0.20
Trigonal Planar $^{11}BO_3$ (non-Ring)	2.55 MHz	0.20
Tetrahedral $^{11}BO_4$ (1B,3Si)	0.30 MHz	0.00
Tetrahedral $^{11}BO_4$ (0B 4Si)	0.30 MHz	0.00

Lin-Shu Du and Jonathan F. Stebbins, *J. Non-Cryst. Solids* **315** (2003) 239–255

Point Charge Model for Predicting Electric Field Gradients

Bent

Place quadrupole nucleus at the origin with z-axis in plane containing atoms and perpendicular to the angle bisector

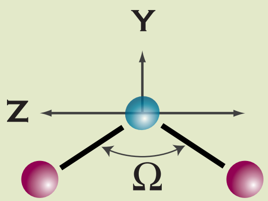

$$\langle R_{2,0}\rangle = \frac{Ze}{d^3}(3\sin^2\Omega/2 - 1), \quad \langle R_{2,\pm 1}\rangle = 0, \quad \text{and} \quad \langle R_{2,\pm 2}\rangle = \frac{Ze}{d^3}\sqrt{\frac{3}{2}}\cos^2\Omega/2$$

$$C_q = 2\frac{e^2Q}{h}\frac{Z}{d^3}(1-\cos\Omega) \quad \text{and} \quad \eta = -\frac{3(\cos\Omega + 1)}{3\cos\Omega - 1}$$

^{17}O quadrupolar coupling parameters in Si-^{17}O-Si linkage as a function of Si-O-Si angle

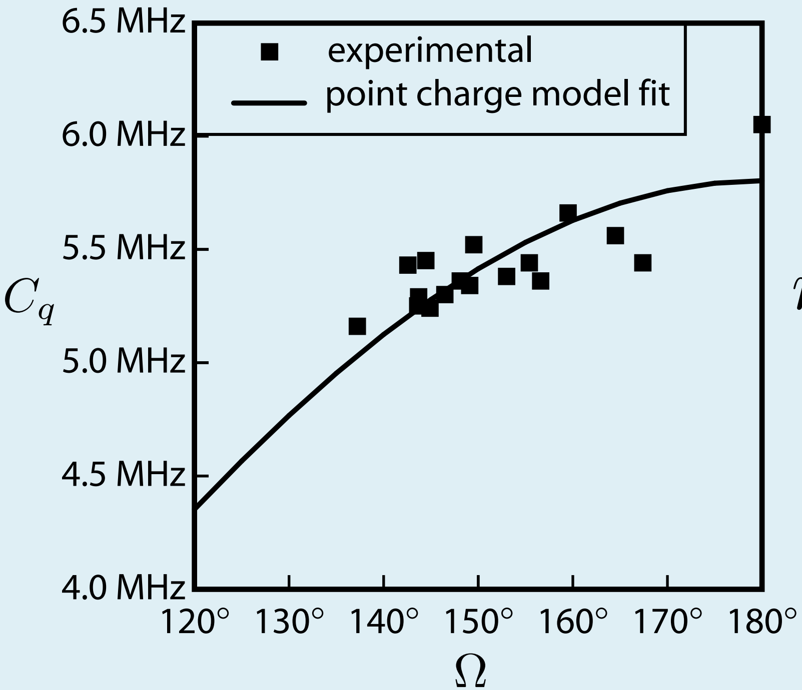

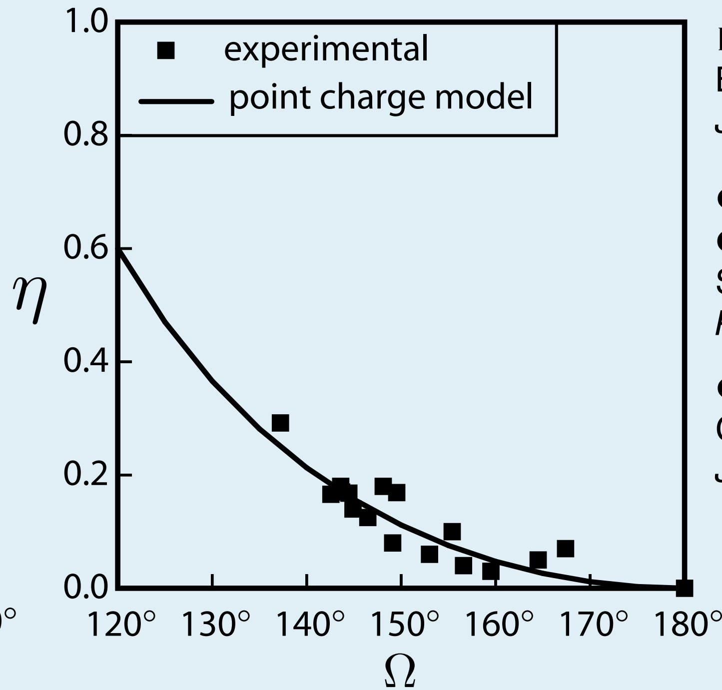

Ferrierite - 10 sites
Bull et al,
J. Am. Chem. Soc. **122** (2000) 4948

Cristobalite - 1 site
Quartz - 1 site
Spearing et al,
Phys. Chem. Min. **19** (1992) 307

Coesite - 5 sites
Grandinetti, et al,
J. Phys. Chem. **99** (1995) 12341

Rough Guide to Some Point Charge Models for EFG

Name	Structure	C_q	η_q
linear (1)	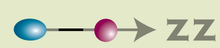	$2\frac{e^2Q}{h}\frac{Z}{d^3}$	0
linear (2)	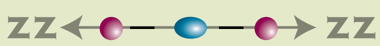	$4\frac{e^2Q}{h}\frac{Z}{d^3}$	0
bent (2)	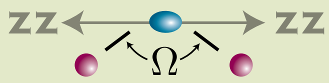	$2\frac{e^2Q}{h}\frac{Z}{d^3}(1-\cos\Omega)$	$-\frac{3(\cos\Omega+1)}{3\cos\Omega-1}$
Trigonal Planar (3)	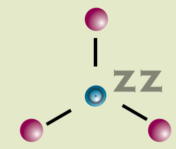	$-3\frac{e^2Q}{h}\frac{Z}{d^3}$	0
Tetrahedral (4)	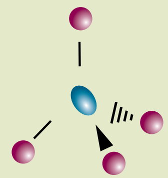	0	0
Trigonal Bipyramidal (5)	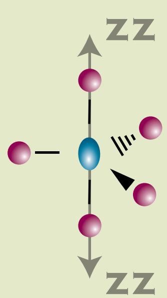	$\frac{e^2Q}{h}\frac{Z}{d^3}$	0
Octahedral (6)	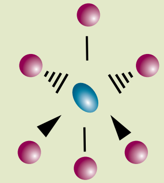	0	0

Nature of M determines ^{17}O Quadrupolar Coupling Constant in M-^{17}O-M linkage

$[(OH)_3M\text{-}O\text{-}M(OH)_3]^{2-}$ where M=B, Al, and Ga

$(OH)_3M\text{-}O\text{-}M(OH)_3$ where M=C, Si, and Ge

$(OH)_2OM\text{-}O\text{-}MO(OH)_2$ where M=P and As

$(OH)O_2M\text{-}O\text{-}MO_2(OH)$ where M=S and Se

M-O-M Angle and MO distance at optimized value

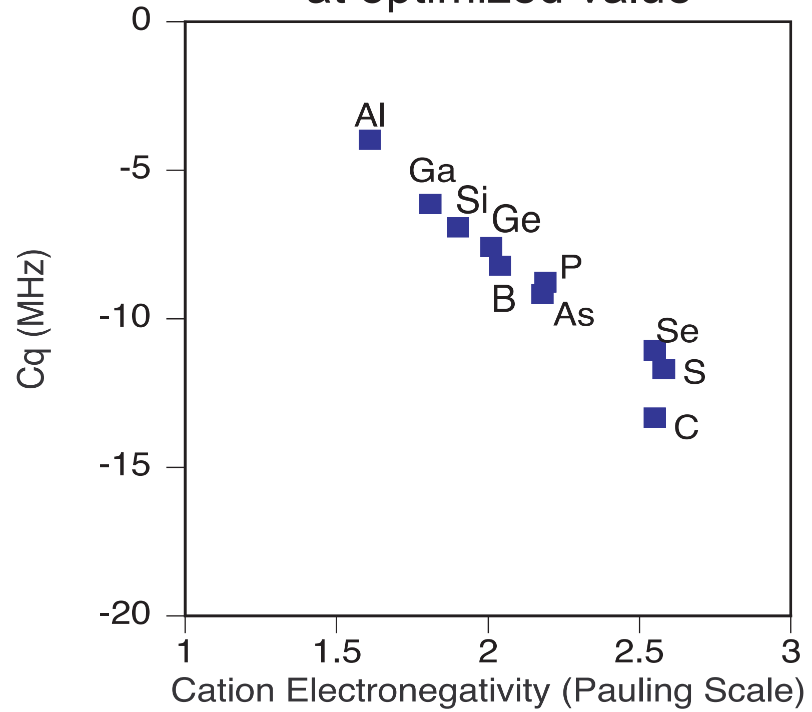

After Oldfield and Co-Workers
JACS, **106**, 2502 (1984), *JACS*, **108**, 7236 (1986)
JPC, **91**, 1054 (1987).

Identical M-O-M angles and MO distances

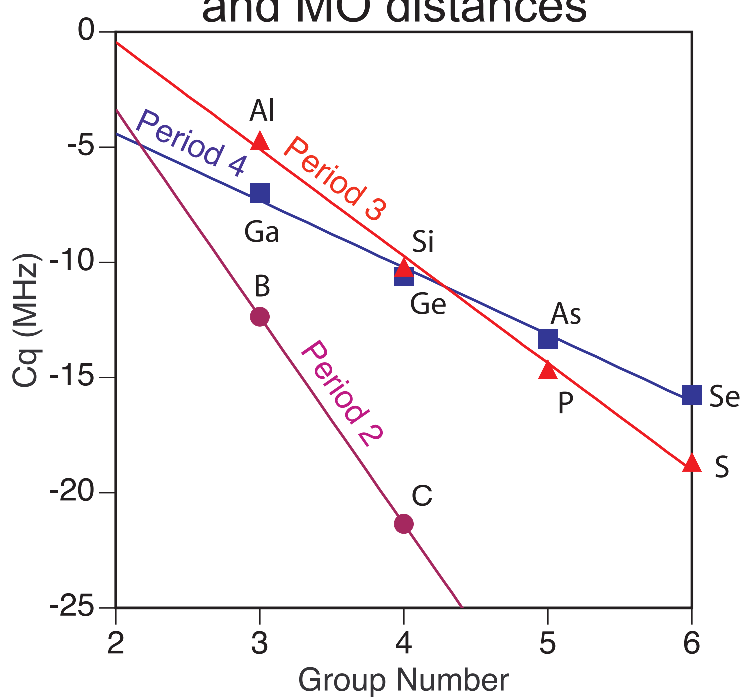

Clark and Grandinetti
SSNMR, **16**, 55 (2000).

Local Geometry is Secondary Factor

How does Local Geometry determine Bridging Oxygen EFG?

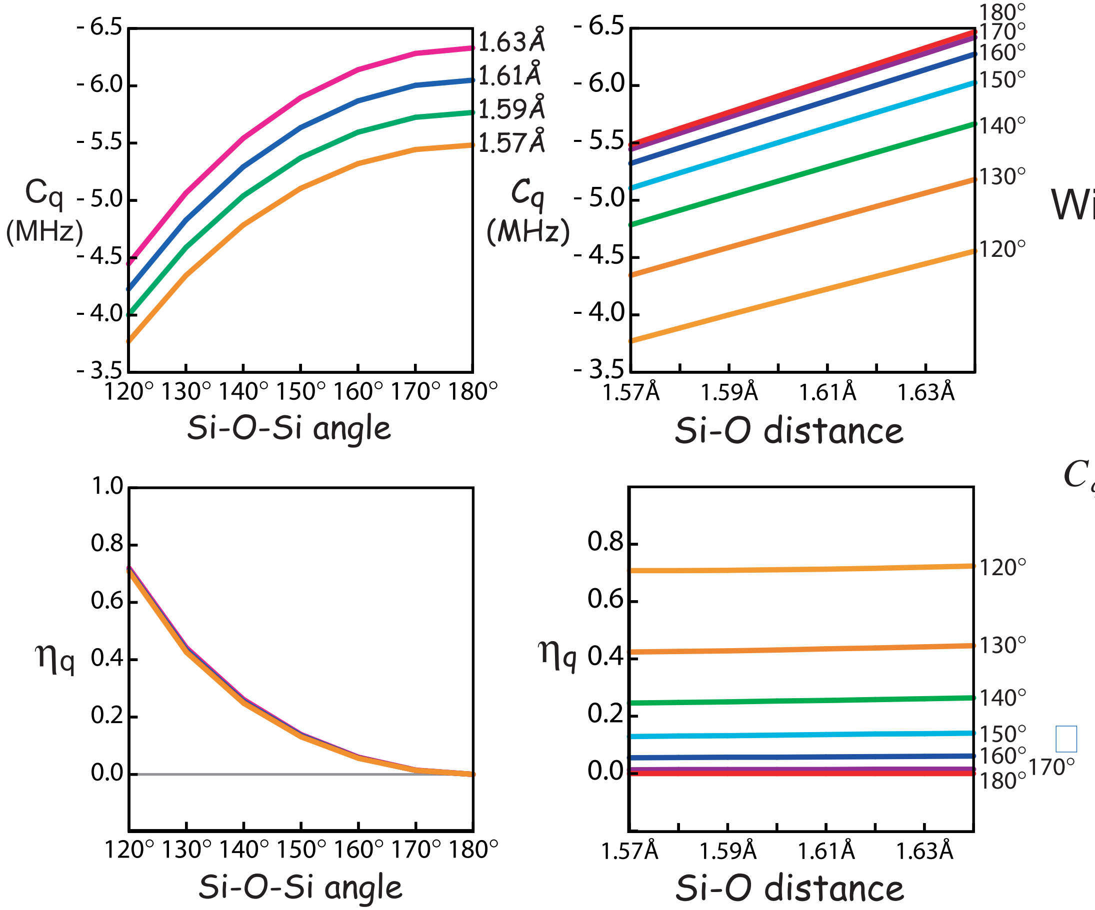

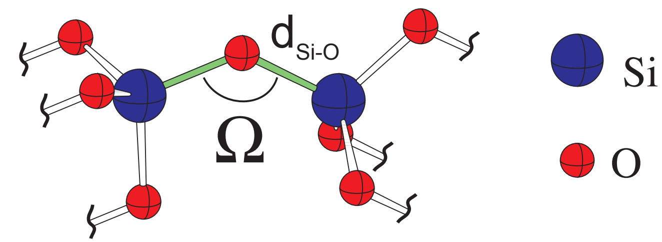

With all other factors constant ...

Bridging Oxygen |Cq| values

- decrease with decreasing Si-O-Si angle
- decrease linearly with decreasing Si-O distance

$$C_q(d_{\text{Si-O}},\Omega)=-(5.91\,\text{MHz})\left(\frac{1}{2}+\frac{\cos\Omega}{\cos\Omega-1}\right)^{1.948}-(15\,\text{MHz/Å})(d_{\text{Si-O}}-1.6\text{Å})$$

Bridging Oxygen η_q values

- increase with decreasing Si-O-Si angle
- are nearly independent of Si-O distance

$$\eta_q(\Omega)=5.03\left(\frac{1}{2}-\frac{\cos\Omega}{\cos\Omega-1}\right)^{1.09}$$

Clark and Grandinetti, *J. Phys. Condensed Matter,* **15**, S2387-S2395,(2003)

Quadrupolar Coupling Parameters can be used to measure Angles and Distances

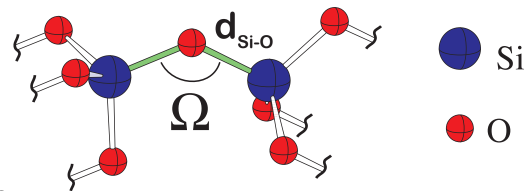

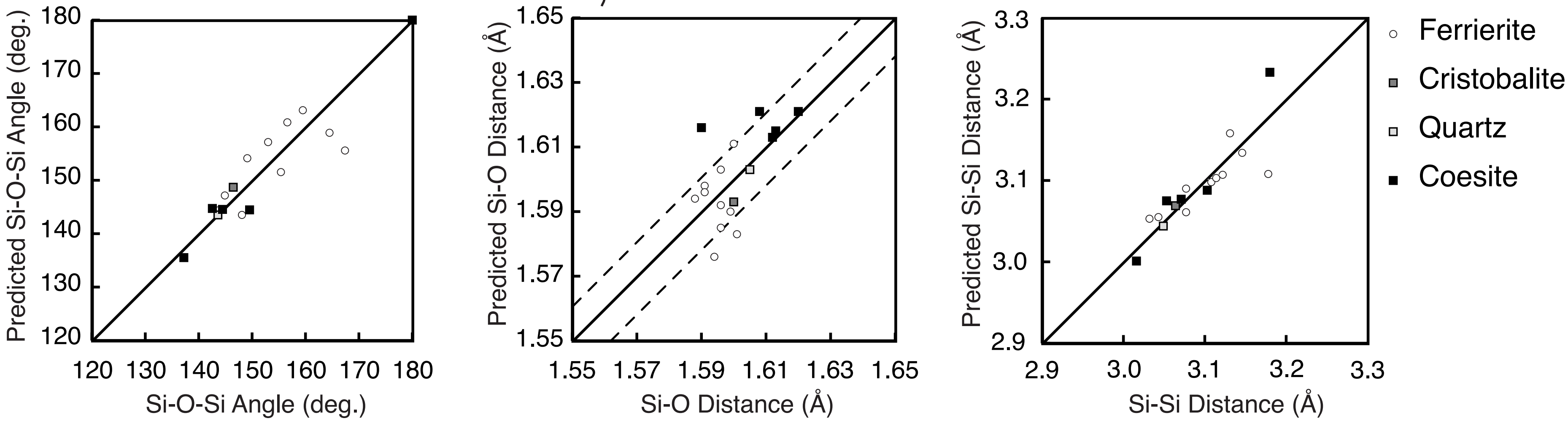

And Their Correlations

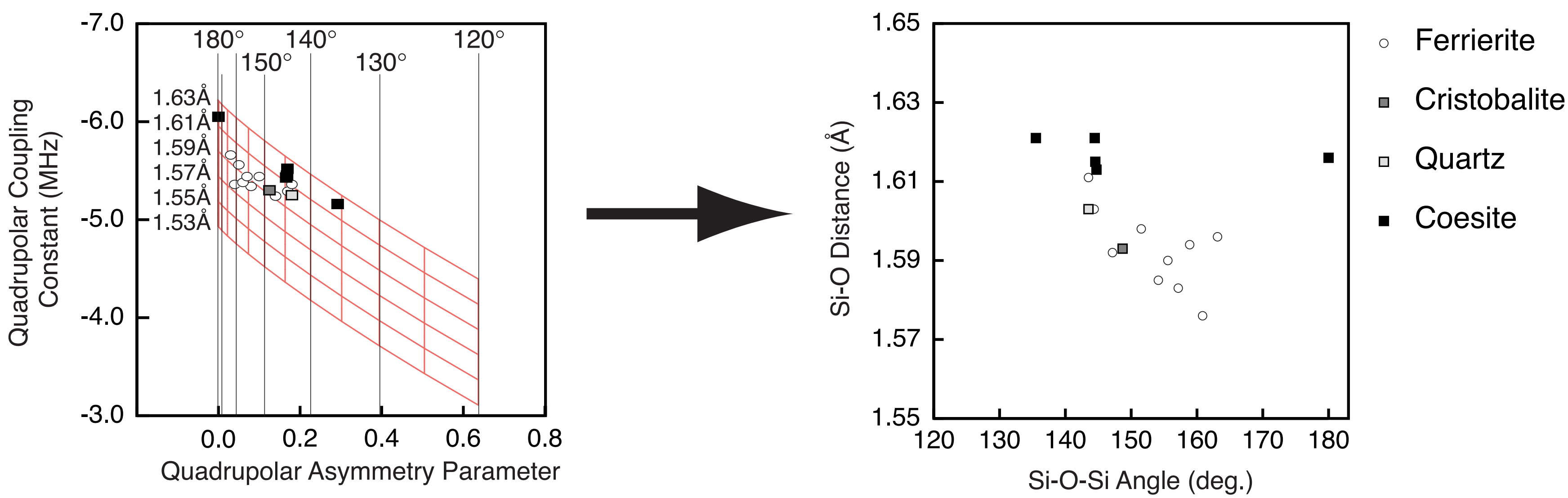

RAPT Enhanced ^{17}O DAS of SiO_2 Glass

Clark, Grandinetti, Florian, Stebbins, *Phys. Rev. B*, **70**, 064202 (2004).

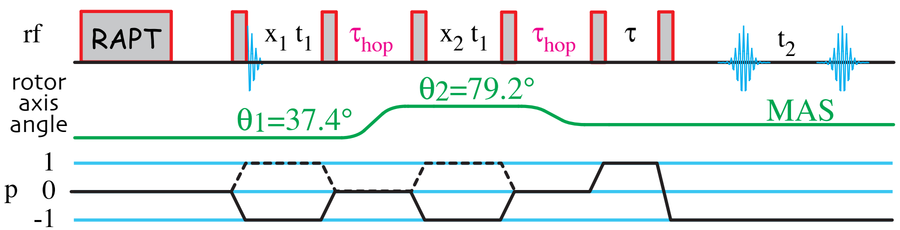

Spectrum taken at 9.4 Tesla

Selected Cross-Sections and Best Fit Simulations

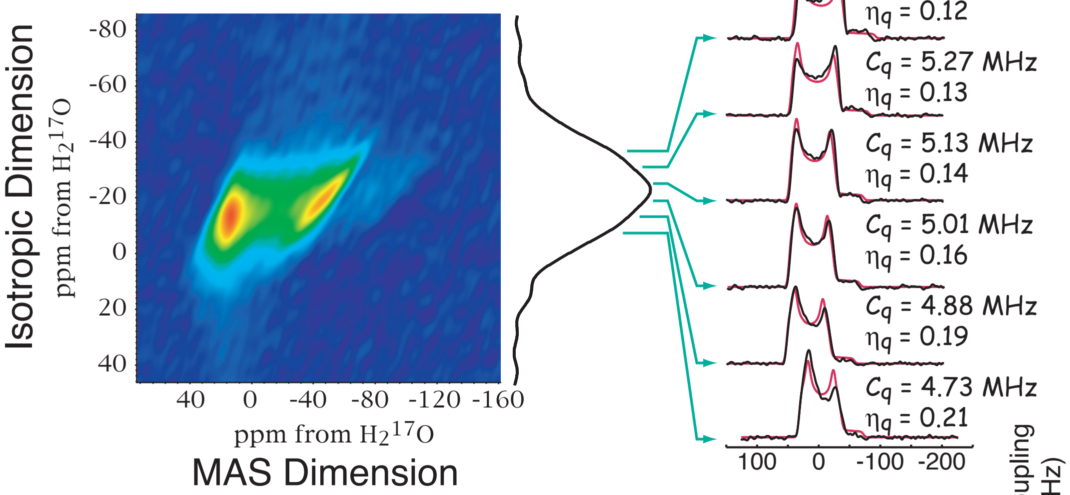

Least Squares Fit

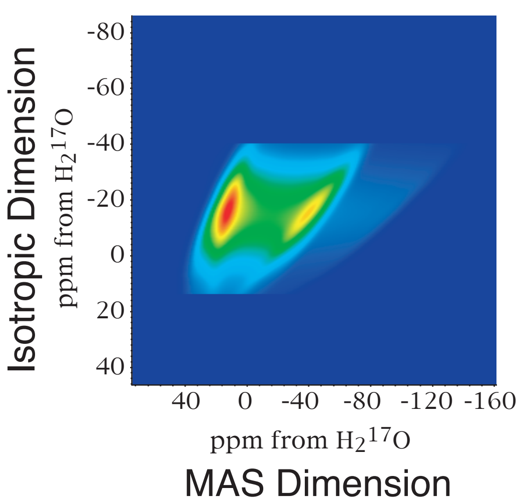

Residuals

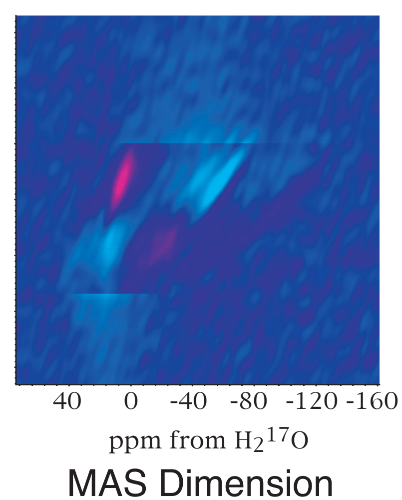

Distribution and Correlation of ^{17}O NMR Parameters in SiO_2 Glass

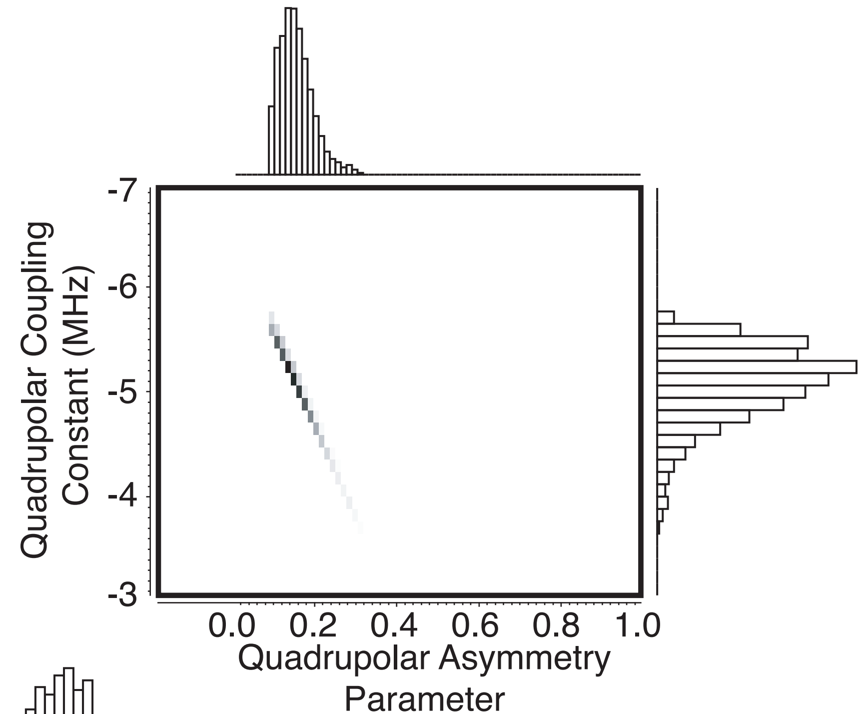

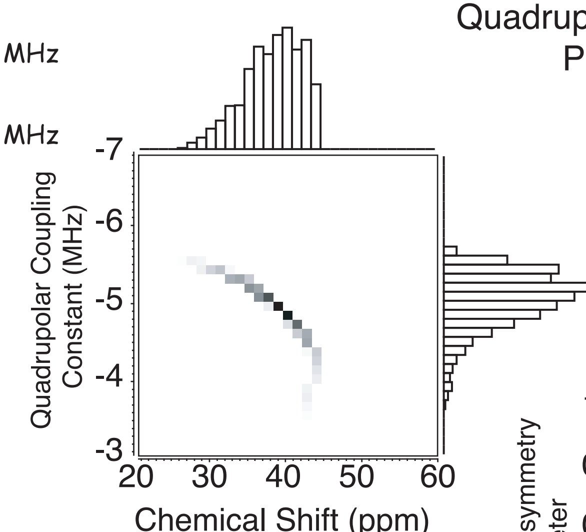

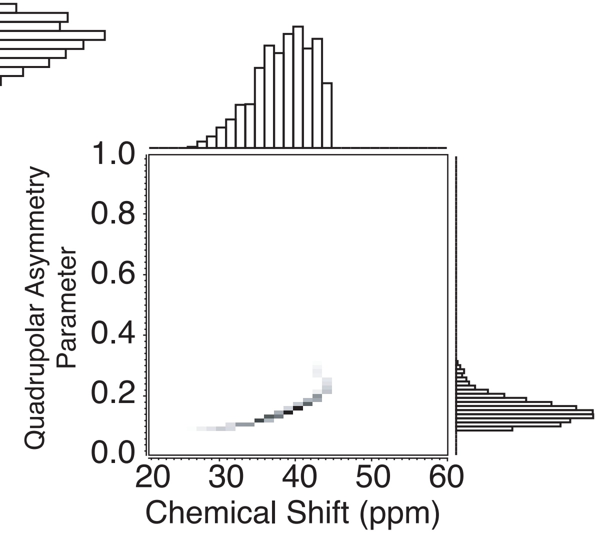

Si-O-Si Angle And Distance Distributions in Silica Glass from Cq and ηq

Clark, Grandinetti, Florian, Stebbins, *Phys. Rev. B*, **70**, 064202 (2004).

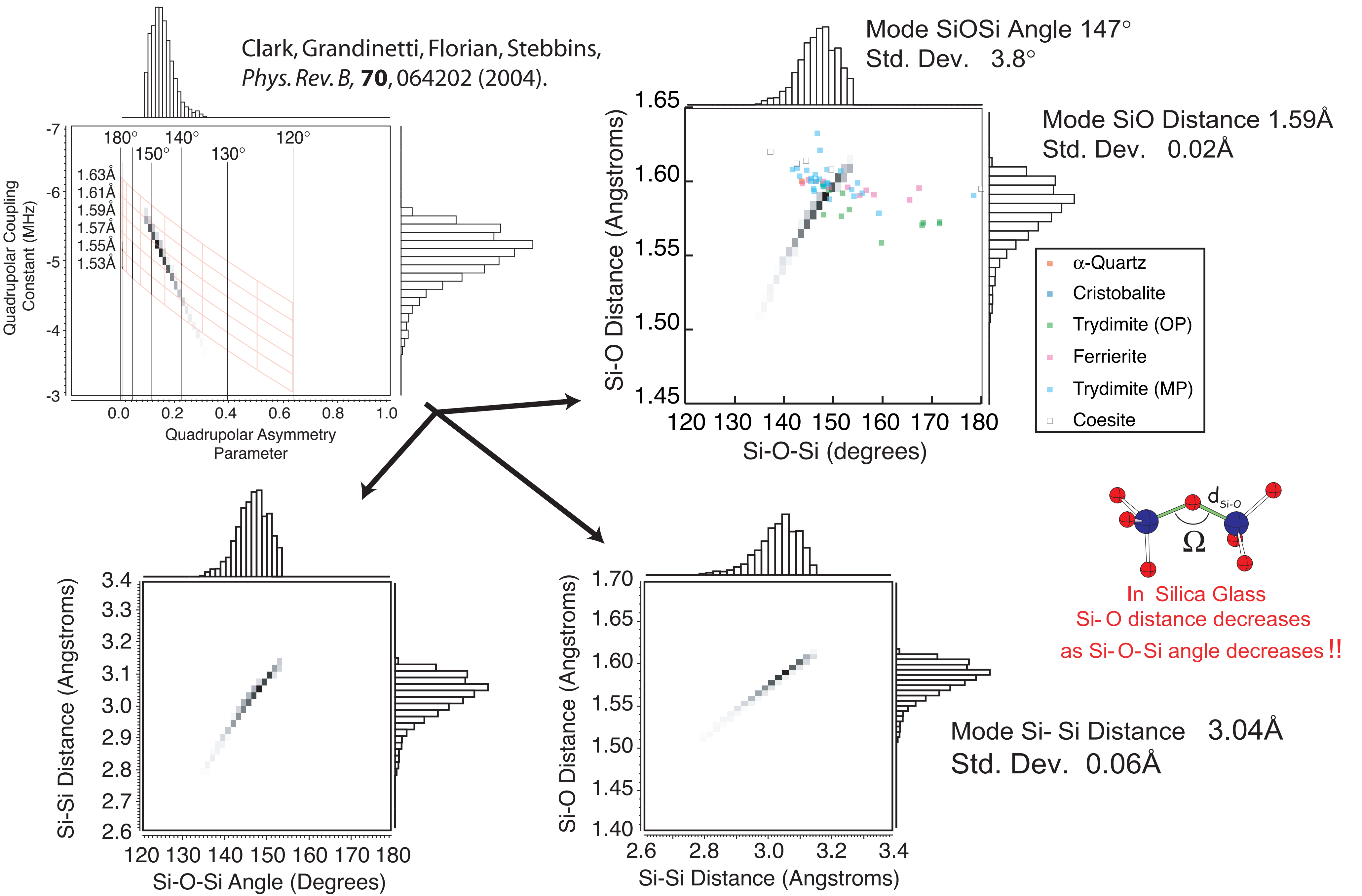

In Silica Glass
Si- O distance decreases
as Si- O- Si angle decreases !!

Comparison of Modified NMR Distance Distributions with X-ray

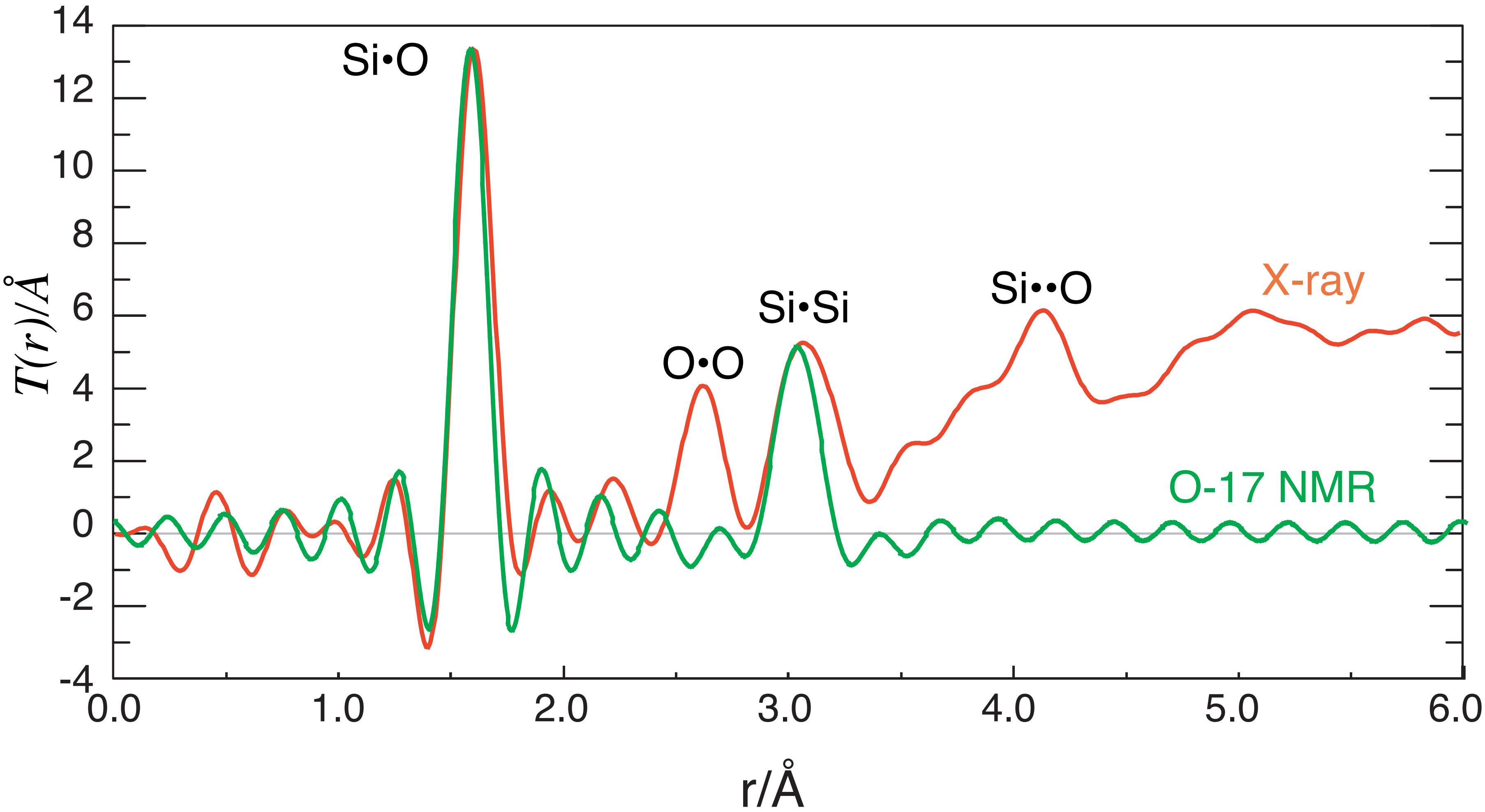

Clark, Grandinetti, Florian, Stebbins, *Phys. Rev. B*, **70**, 064202 (2004).

Acknowledgements

Current Group

Nicole Trease
Jason Ash
travis Sefzik
Krishna Kishor-Dey
Samantha Farley

Past Group Members

Pierre Florian
Alex Klymachyov
Ted Clark
Subramanian Prasad
Karl Vermillion
Ping Zhang
Zhi Yao
Hyung-Tae Kwak
Ramesh Sharma

"Quadrupole" Collaborators

Alex Pines, Jay Baltisberger, Antoine Llor, Margaret Eastman, Young Lee, Boqin Sun, Yue Wu, Jonathan Stebbins, Ian Farnan, Ulrike Werner-Zwanziger, Sheryl Gann, Josef Zwanziger, Joe Sachleben, Maurice Goldman, Zbigniew Olejniczak, Andrew Kolbert, Lucio Frydman, Gerry Chingas, Raz Jelinek, Brad Chmelka, Jacek Klinowski, Dominique Massiot, Joseph Virlet, Zhehong Gan, Thomas Vosegaard, Lyndon Emsley, Dimitri Sakellariou, Todd Lowary, Michael Deschamps, Franck Fayon, Stefan Steuernagel

The Ohio State University

National science Foundation